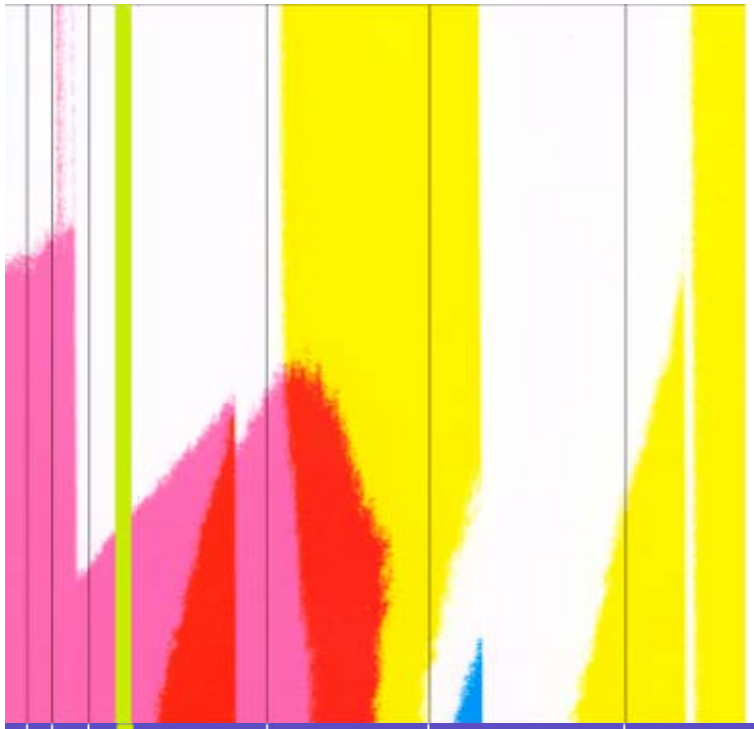

Computational Models of Human Organs

Olivier Clatz
Hervé Delingette

INSTITUT NATIONAL
DE RECHERCHE
EN INFORMATIQUE
ET EN AUTOMATIQUE

INRIA
SOPHIA ANTIPOLIS

Virtual Human

Development of computational models of the human body driven by :

- Better Understanding of biology and physiology at different scales
- New *in vivo image modalities* of the human body
- Fast Growth of computer technology and computer science

Global modeling of the human body

Physiome Project

International consortium

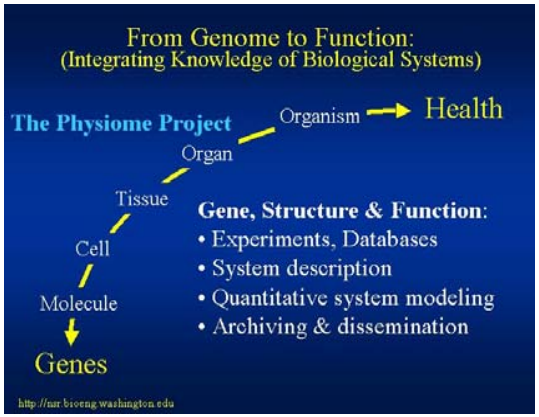

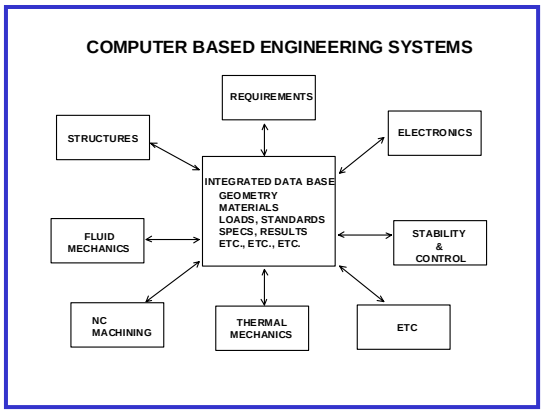

Digital Human

International consortium

Visible Human

NLM, USA

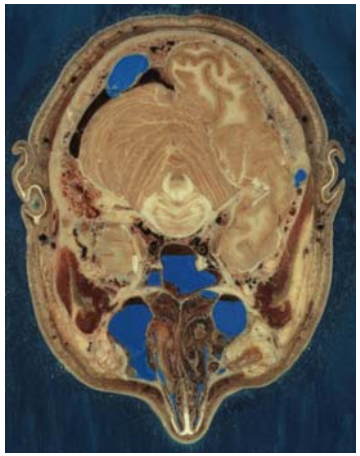

ESI Group

Virtual Dummies for crash tests

Modeling Levels

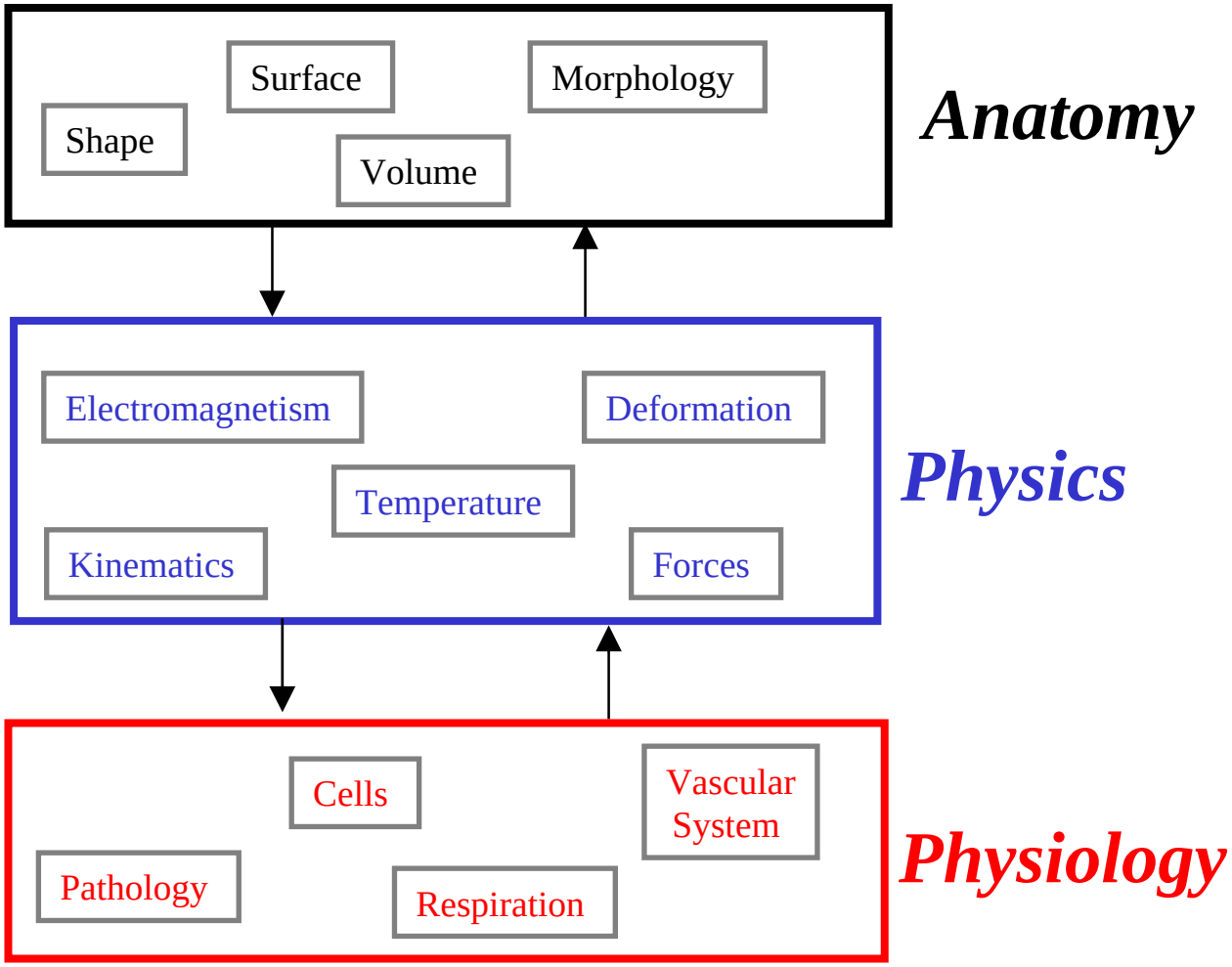

Anatomy

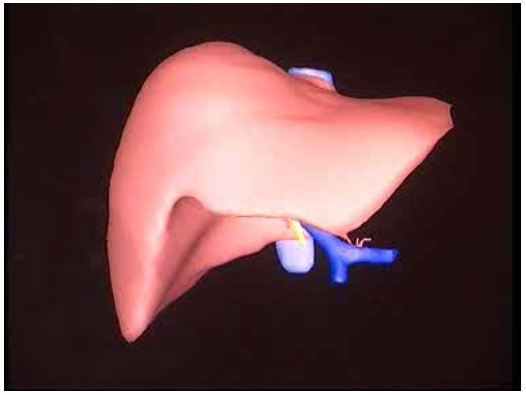

Physics

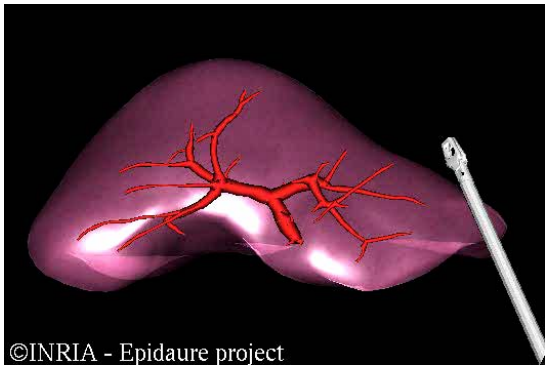

Physiology

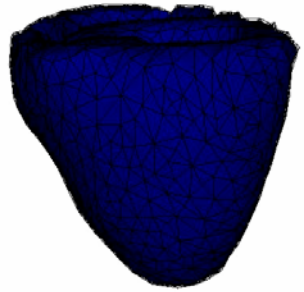

Modeling and Imaging

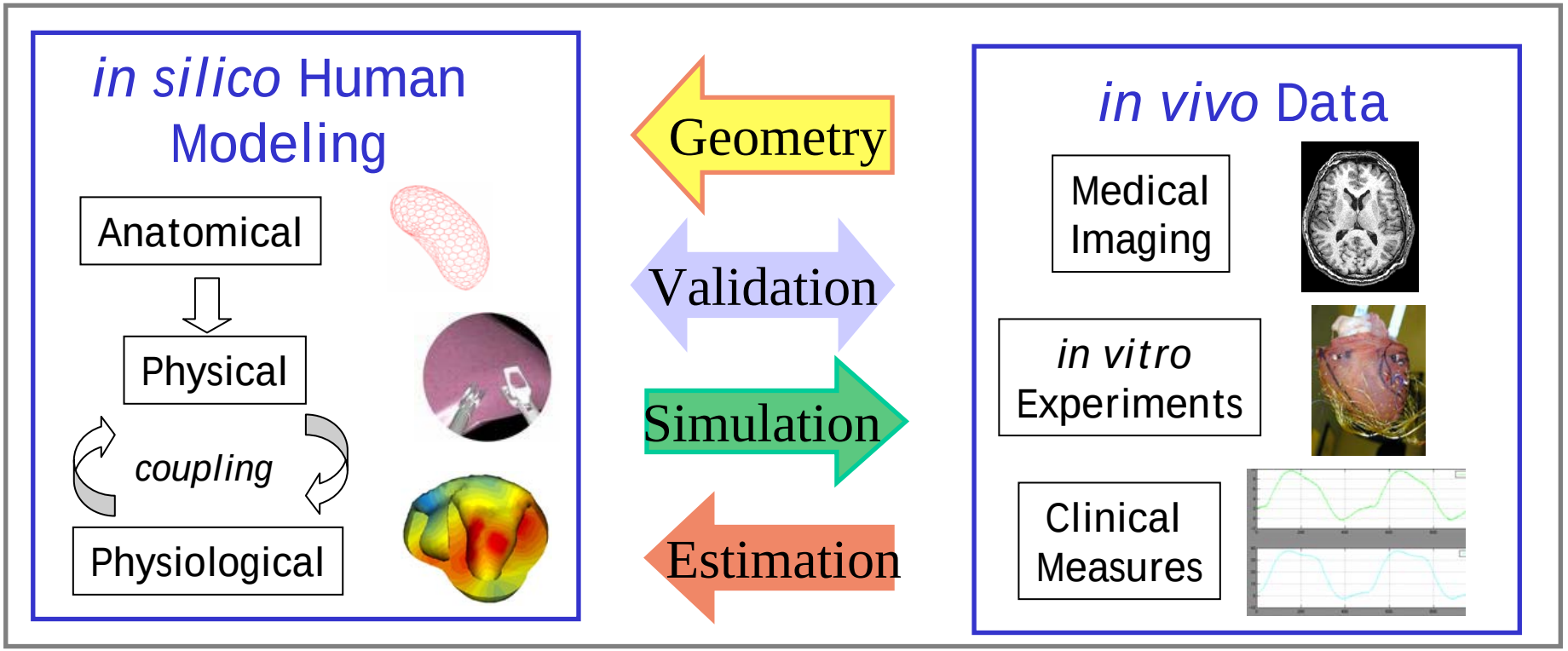

Mesh construction from medical images

Combining Images and Models

- **1st Goal**: Validation Quantitative Models
  - Reach a better understanding of human physiology and pathology by comparing measured and computed physical values
- **2nd Goal:** Assessment of physical parameters (diagnosis)
  - Guess physical parameters (pressure, speed, stress) by assuming that the physical behavior and boundary conditions are known
- **3rd Goal** : Prediction of physical behavior (therapy)
  - Predict anatomy based on the modeling of a physical phenomenon occurring during therapy (brain shift, cranofacial surgery)

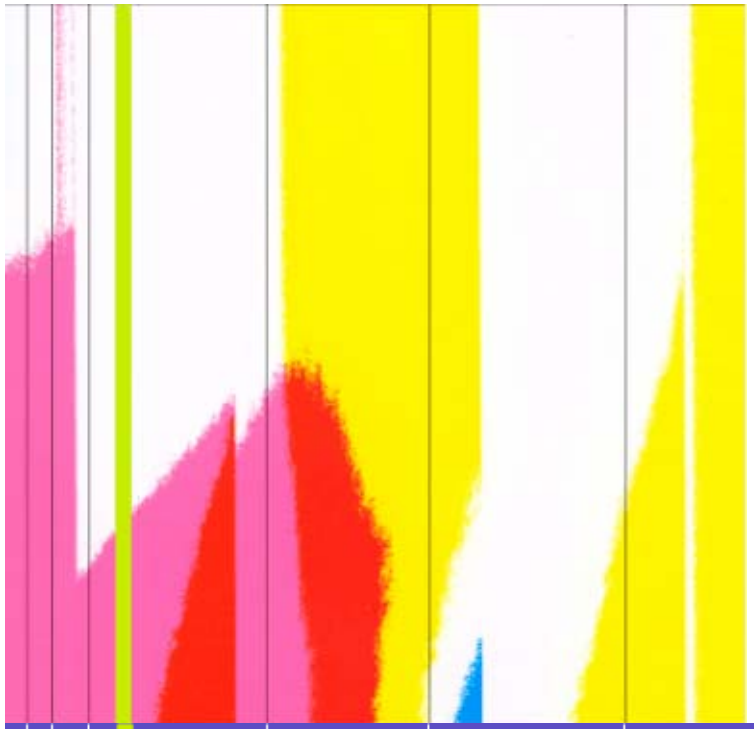

Biomechanical Modeling of the brain

INSTITUT NATIONAL
DE RECHERCHE
EN INFORMATIQUE
ET EN AUTOMATIQUE

INRIA
SOPHIA ANTIPOLIS

Problem position

Despite MRI precision, anatomical structures deform during the operation. (Brain shift)

Decrease of precision compared to the pre-operative planning

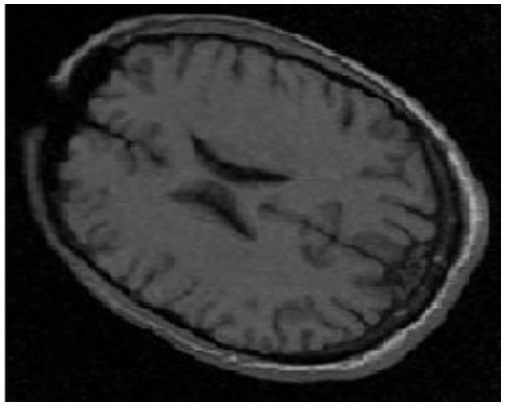

Pre-operative MRI (SPL)

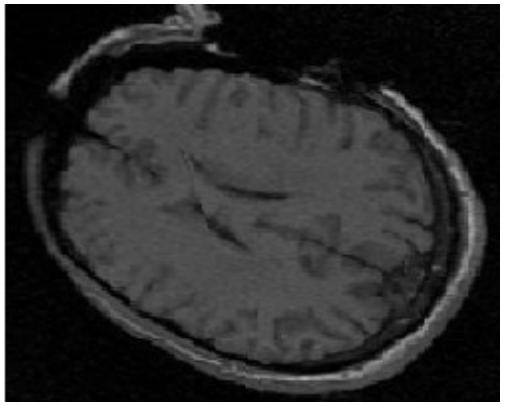

Per-operative MRI (SPL)

Other applications

The Parkinson Disease Procedure

- Stereotactic surgery
- Almost non invasive technique
- Deep implantation of electrodes
- 6 to 10 hours long

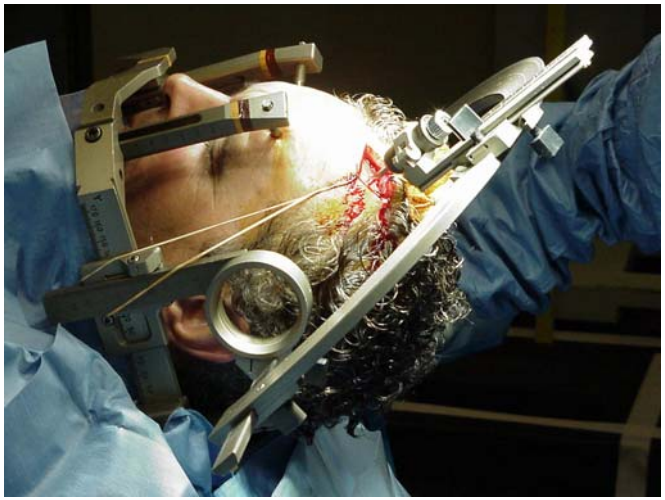

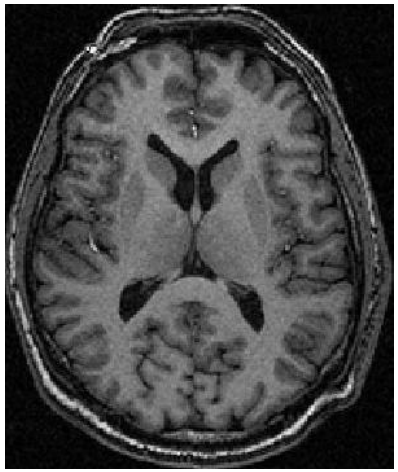

Pre operative MRI (La pitié Salpétriere Hospital Paris)

Post operative MRI (La pitié Salpétriere Hospital Paris)

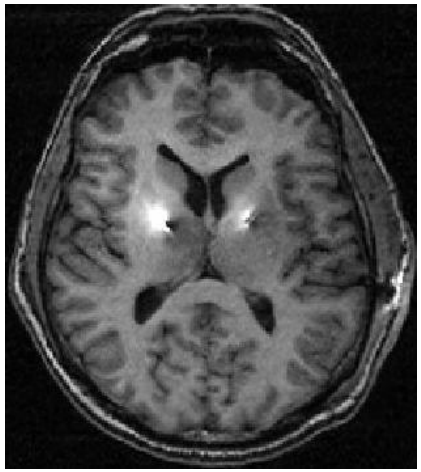

Our approach

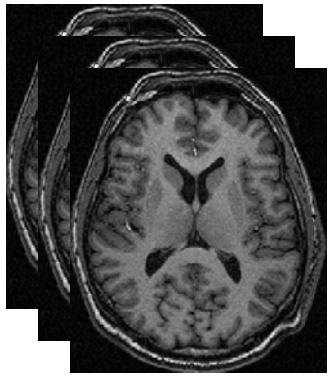

7 patients pre and post operative MRIs

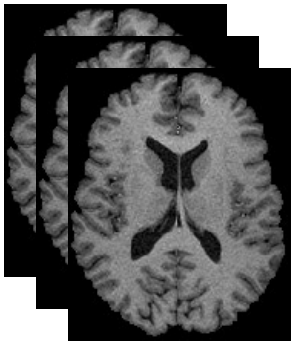

Pre processing : Cortex segmentation

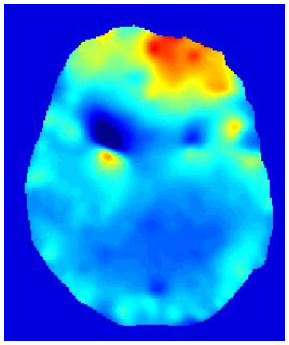

Deformation analysis

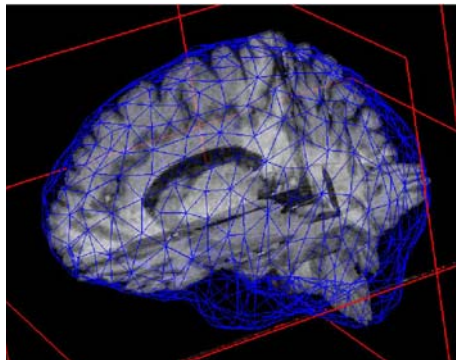

Mesh generation

Characteristic features and **force** boundary conditions

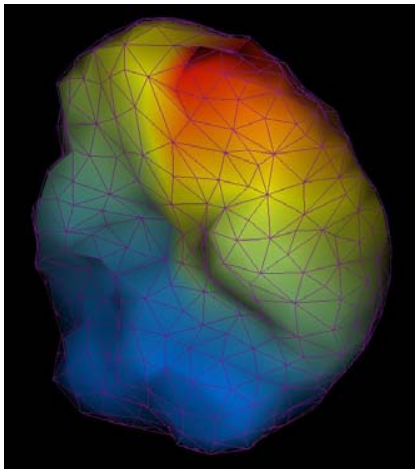

Biomechanical simulated deformation

Image Processing

Cortex segmentation

Atlas deformation-based method

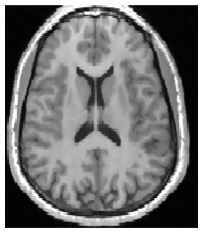

Rigid registration -> non-rigid registration

Measured deformation T(A->I)

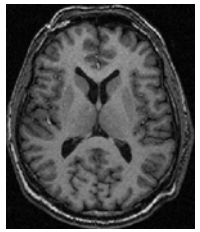

Atlas (A) (Kikinis)

MRI to segment (I)

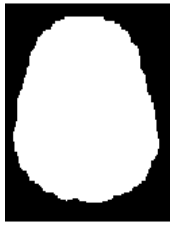

T(A->I)

M '.*I

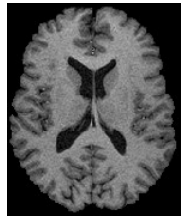

Cortex mask (M)

Deformed mask (M ')

Segmented cortex

Automatic

Precision

Displacement Estimation

Non-rigid registration algorithm “Pasha” (Cachier 2001)

Hypothesis 1: Points with the same grey level should matched

Hypothesis 2: Displacement field should be smooth

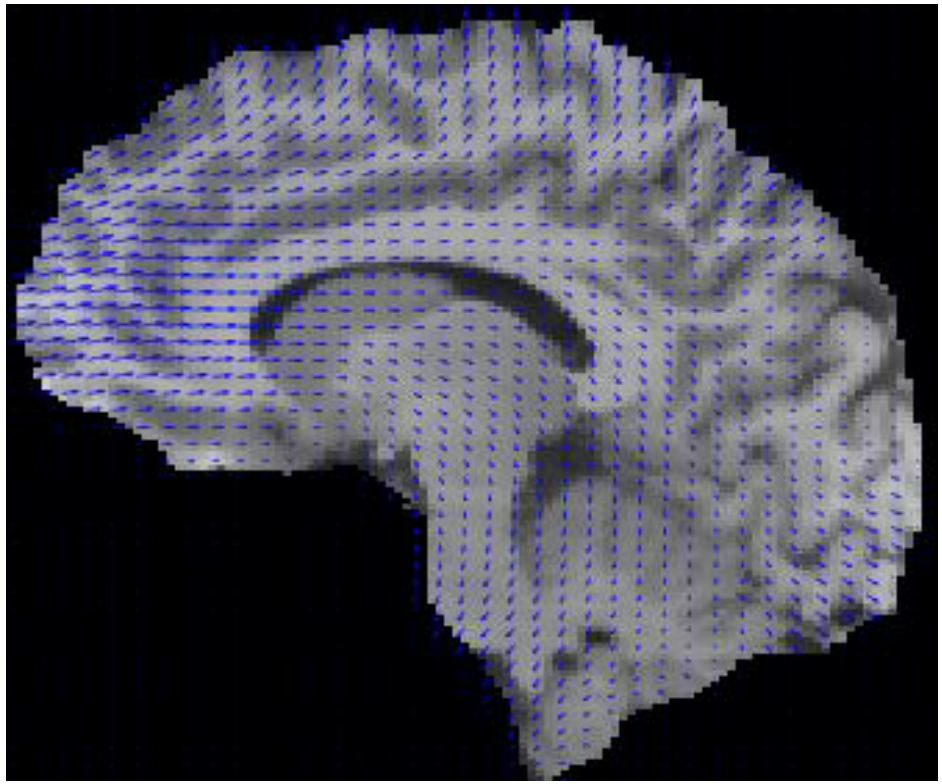

Displacement Field U(X)

Deformation analysis

Local deformation rate

With F the transformation gradient

$$F = \nabla\Phi(X) = \nabla U(X) + Id$$

The volumetric deformation rate is given by :

$$\frac{d\Omega - d\Omega_0}{d\Omega_0} = \det(F) - 1$$

Global *incompressible* comportment: $|\det(F)-1|<0,05$

Electrodes really disturb deformation analysis

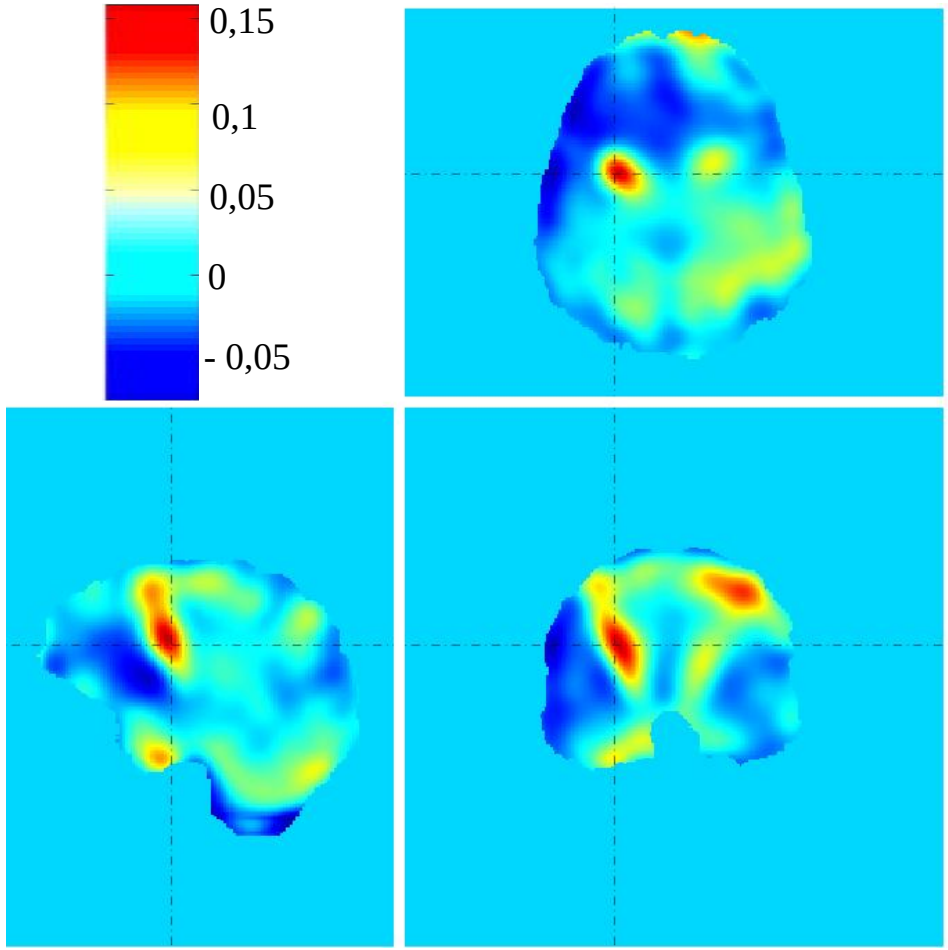

det(*F*)-1

Displacement Field analysis

First results :

- Occipital lobe basis does not move
- Displacement direction aligned with gravity
- Observed asymmetry in the displacement field for right and left hemispheres
- Electrodes induce very important artifacts

Biomechanical Model

- State of the art

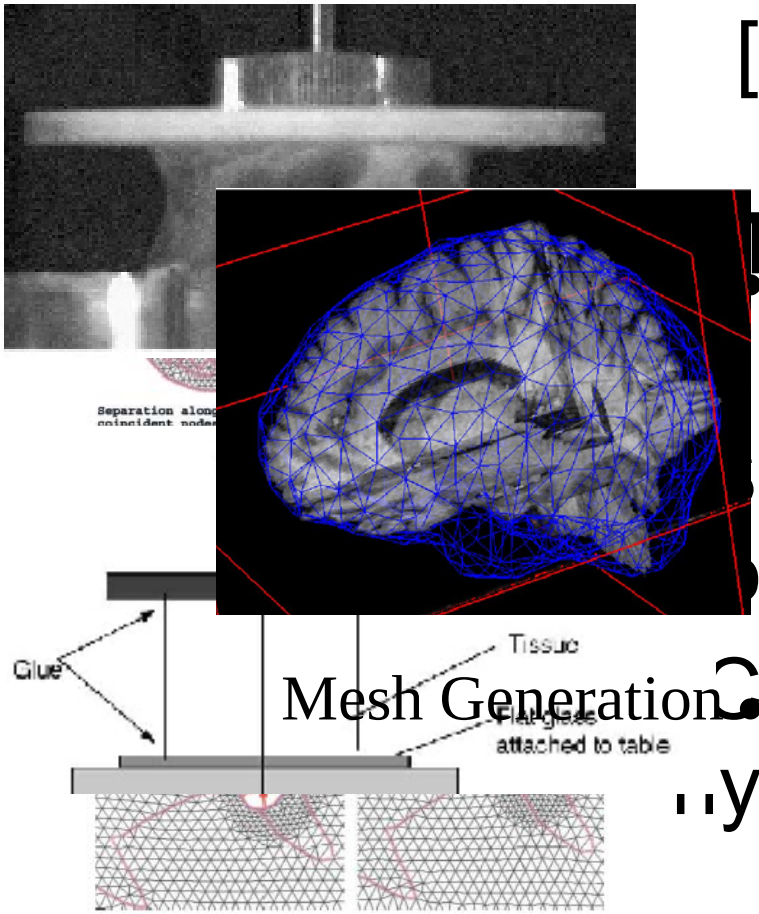

[Miller 1997]

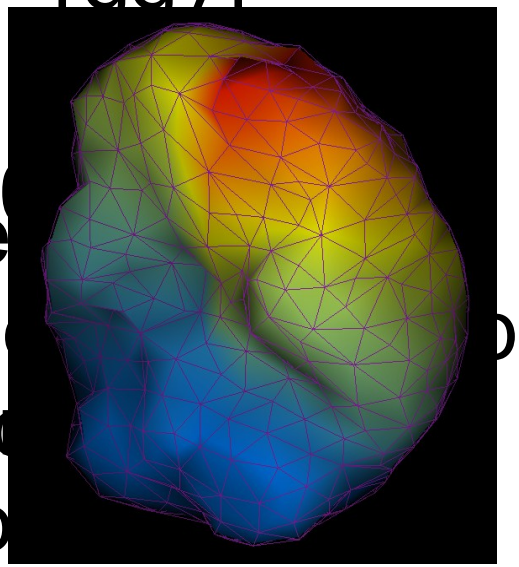

liga 2

Rhe

Expe big

tua

nditio

Mesh Generation Biomechanical Model

Constitutive law

Constitutive law found to be hyper-viscoelastic

yperelastic

The biomechanical model

With respect to the deformation analysis, we

propose the following model :

- Almost incompressible material (u=0.45)
- Brain stiffness chosen according to Miller's in vivo experiments (E = 2000 Pa)
- Vertices at the occipital basis fixed
- Different liquid levels for each hemisphere
- CSF leak induces a gravity volumetric force applied on the emerged part
- Rigid model of the falx cerebri on which vertices slide

The biomechanical model

Left liquid level

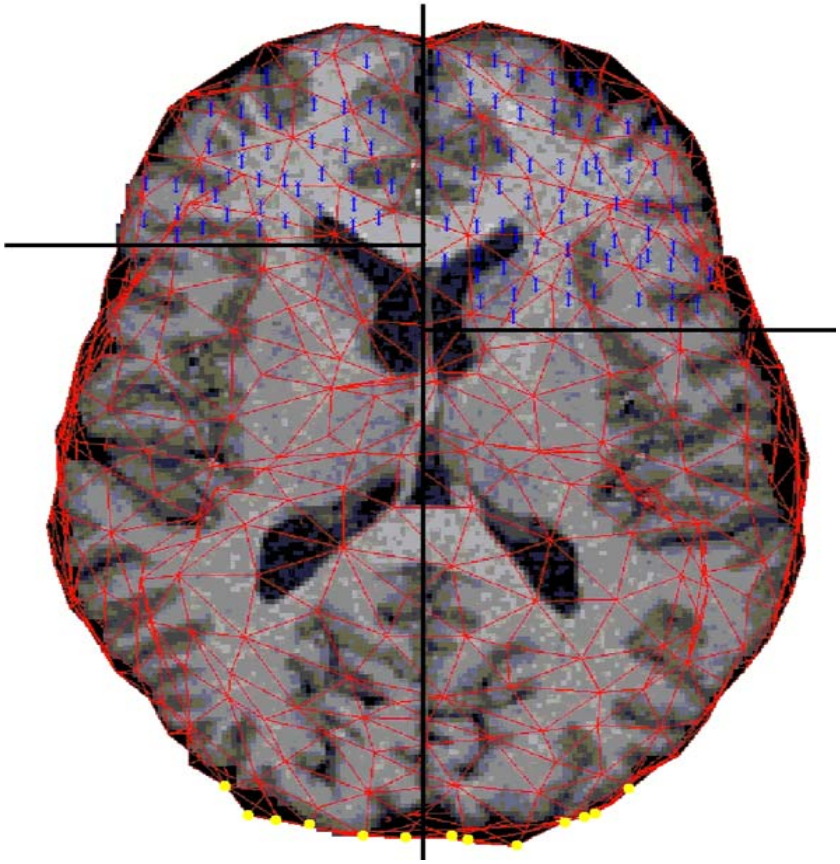

Right liquid level

Gravity

Fixed vertices

Falx cerebri model: vertices slide along the median sagital plane

The biomechanical model

Continuum mechanics and numerical methods :

With defining the linearized Green Lagrange tensor:

$$\varepsilon = \frac{1}{2}(\nabla U + \nabla U^t)$$

The displacement solution of the mechanical problem is a minimization problem :

$$E = \frac{1}{2}\int \varepsilon(\vec{U}) K \varepsilon(\vec{U}).d\Omega - \int \vec{F}\vec{U}.d\Omega$$

The discrete displacement solution of this minimization problem is given by :

$$U = K^{-1}F$$

Comparison Model / Observation

Objectives :

•1) Find CS[illegible]hat best explain the observed deformation[illegible]odel

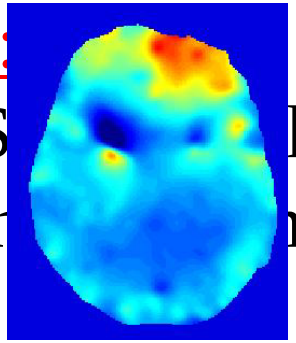

Deformation Analysis

•2) Evaluate the predictive nature of the model

Error Criterion allo[illegible]aluate if the model can explain[illegible] observed deformation:

$$Error = \iiint_{brain\_volume} \left| U_{observed} - U_{predicted} \right|^2 dV$$

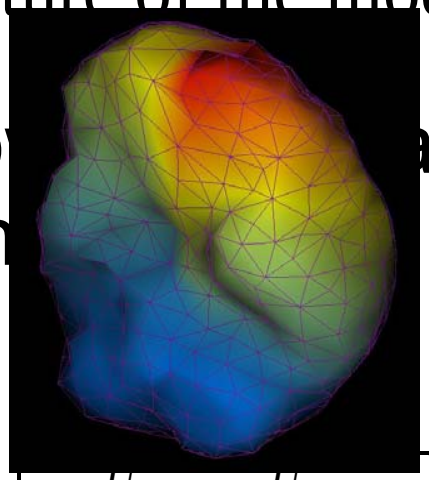

Biomechanical Model

Results

Research of two different liquid level in the skull for each hemisphere :

Error plot as a function of right and left liquid levels in the skull :

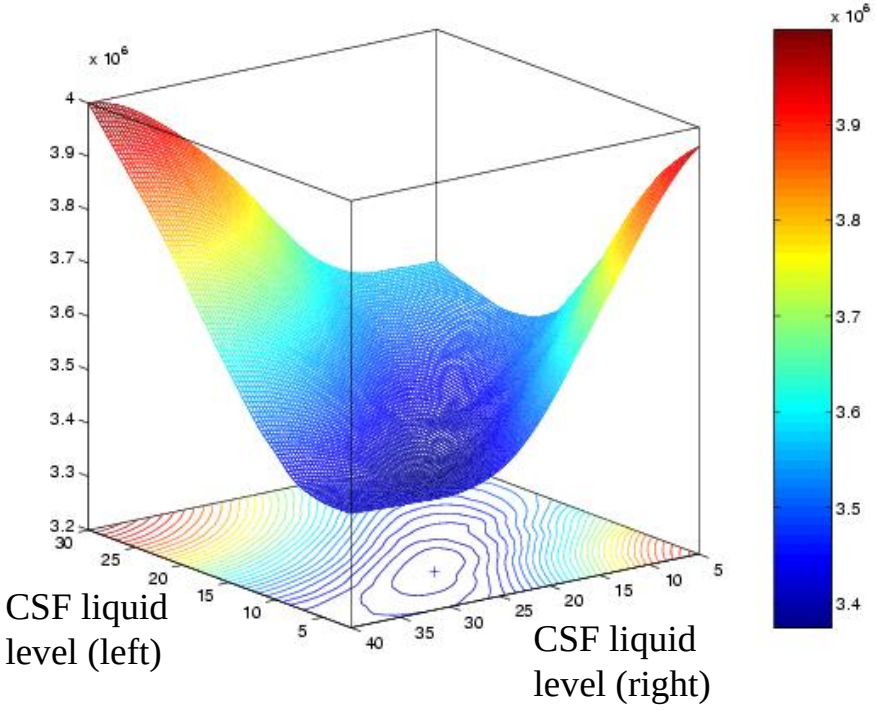

Results

Deformed mesh visualization for optimal left and right liquid levels

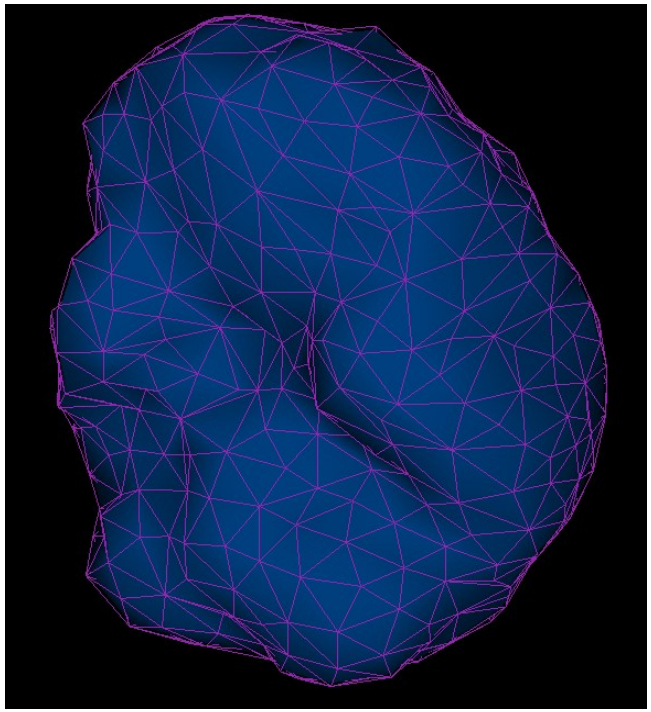

Rest position

8000 tetrahedron

Computation time ~ 1min

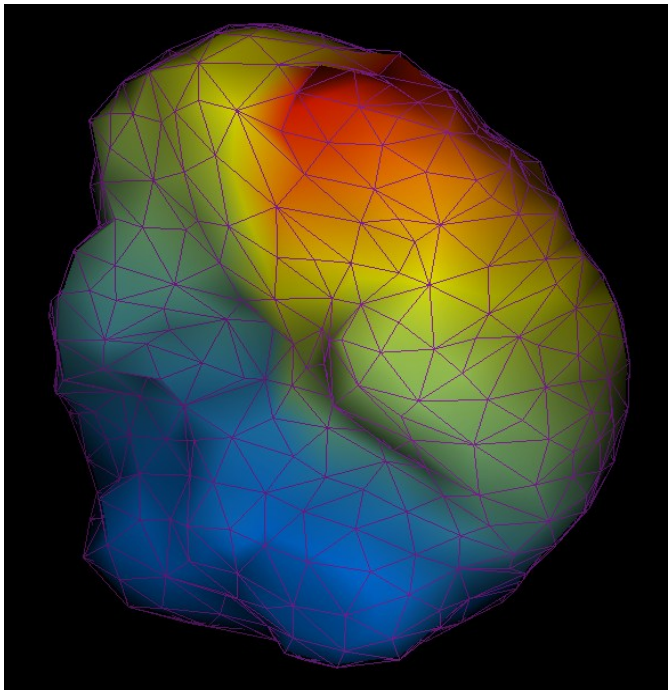

Deformed position

Results

Image difference comparison :

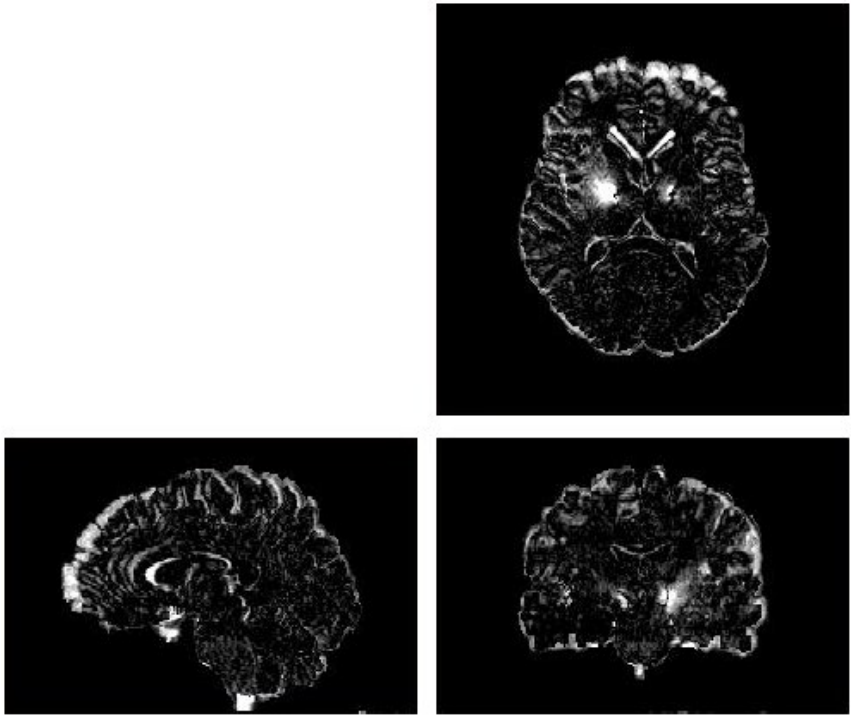

Difference pre/post operative

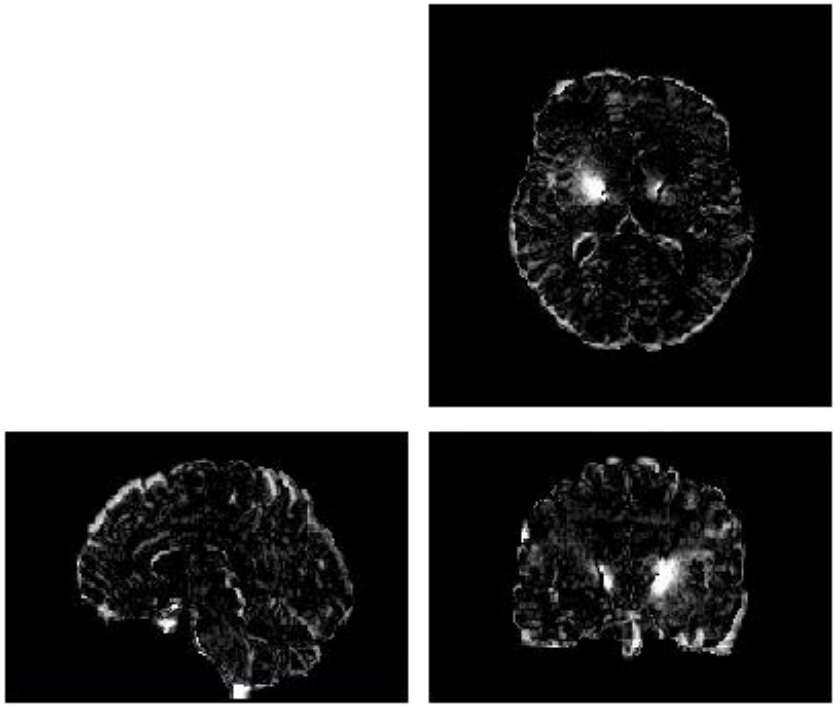

Difference pre-operative/prediction
(for optimal L&R liquid levels)

Results (case with largest displacement)

1. Satisfying displacement in X
2. Error on the temporal lobe
3. Assymetry of displacement in Y
4. Significant electrode-induced artifacts
5. Over-estimated displacement in Z (contact)

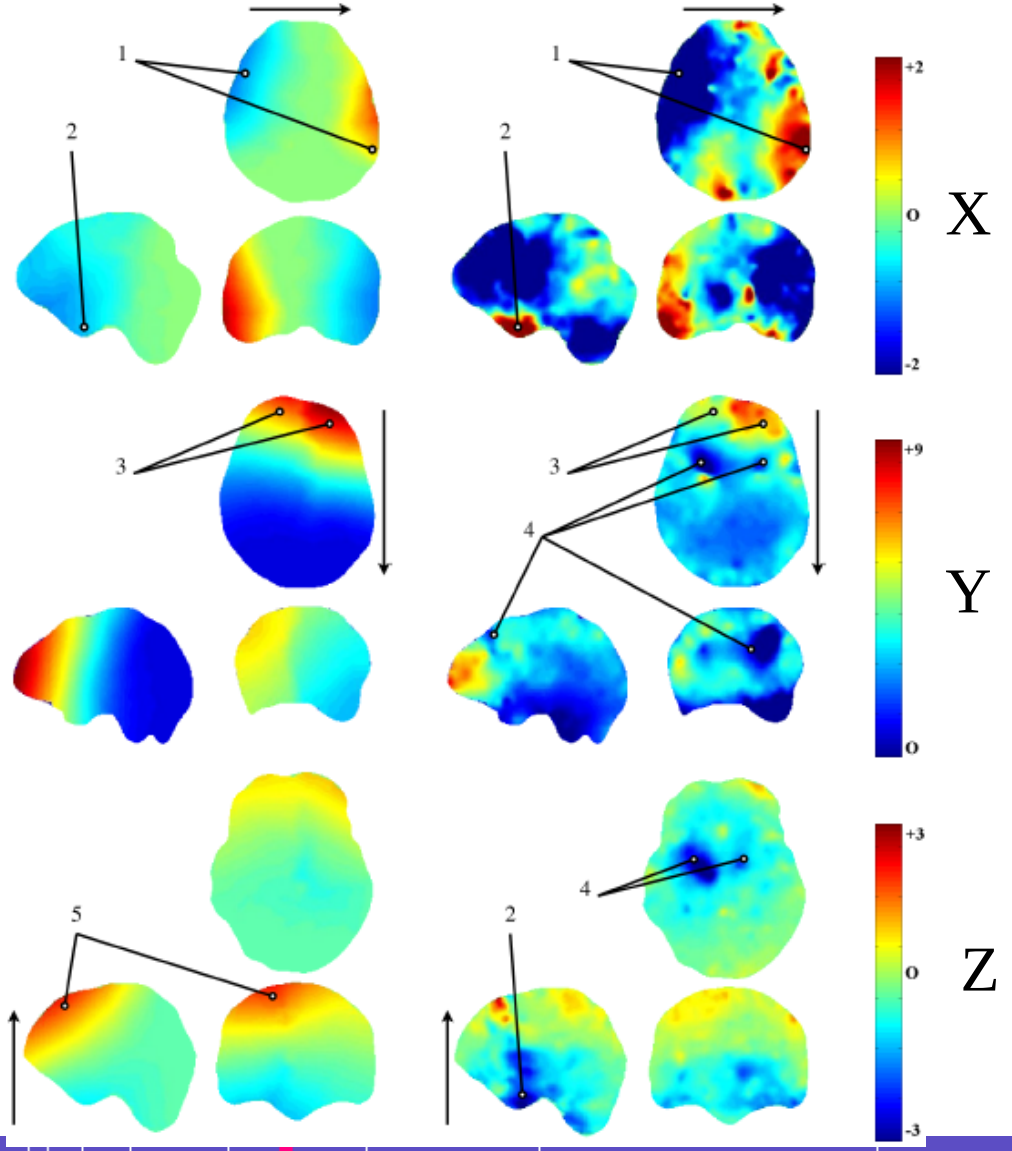

Conclusion

Comparison between predicted and measured CSF levels

+ Ability to predict the global deformation induced the loss of CSF

- Registration must be improved

- Accuracy in the Z direction

- Problems near the cortex surface

Need for a more sophisticated model

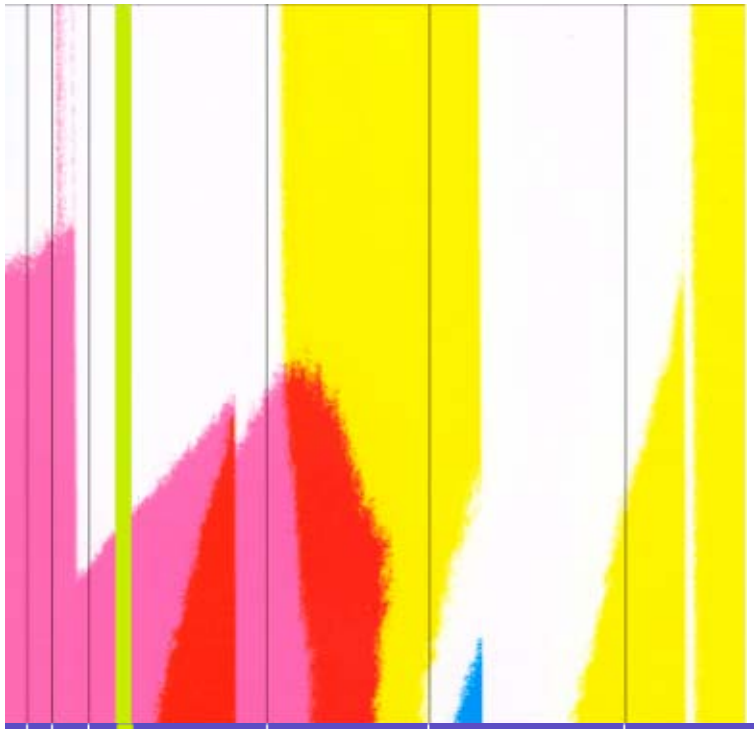

Robust Non-rigid Registration to Capture Brain Shift from Intraoperative MRI

INSTITUT NATIONAL
DE RECHERCHE
EN INFORMATIQUE
ET EN AUTOMATIQUE

INRIA
SOPHIA ANTIPOLIS

Motivation

MR images (T1, T2, DTI, fMRI ...) can be acquired before neurosurgery to localize brain structures (white mater fibers, functional areas, gray nuclei...) with respect to the tumor.

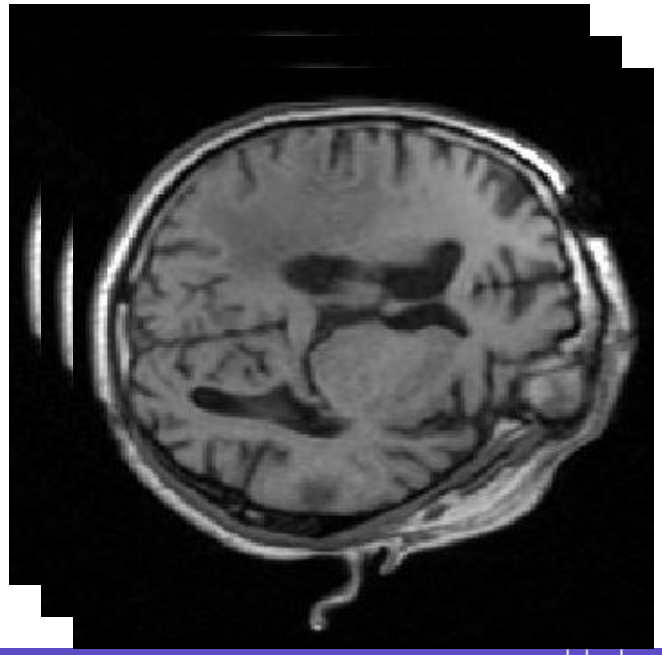

Pre-operative MR T1 weighted image

Motivation

- But… brain deforms during neurosurgery, inducing a localization error with respect to the pre-operative planning.

- However… intra-operative MR scanners allow to image the deformation.

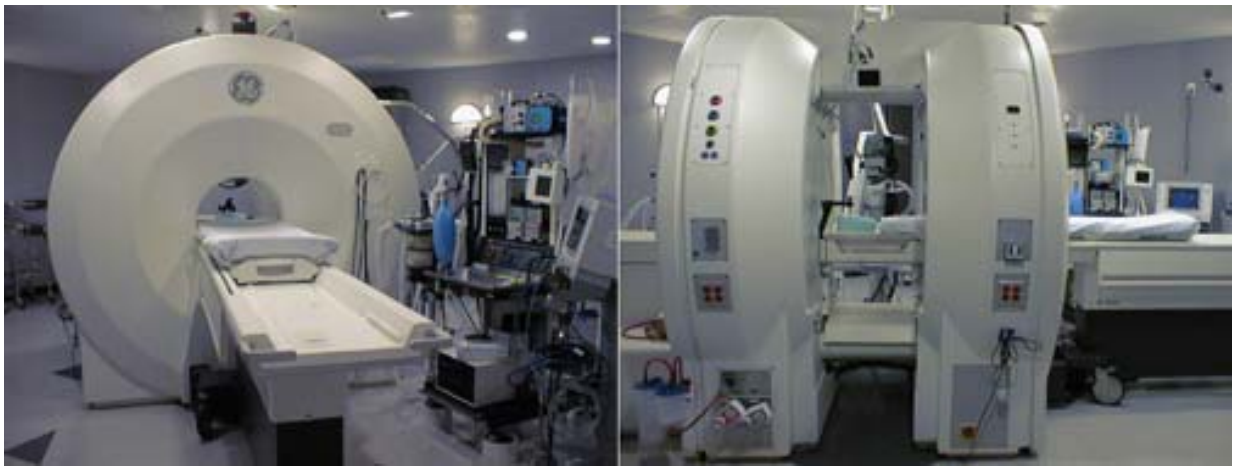

The 0.5 T open magnet system (Signa SP, GE Medical Systems) of the Brigham and Women's Hospital

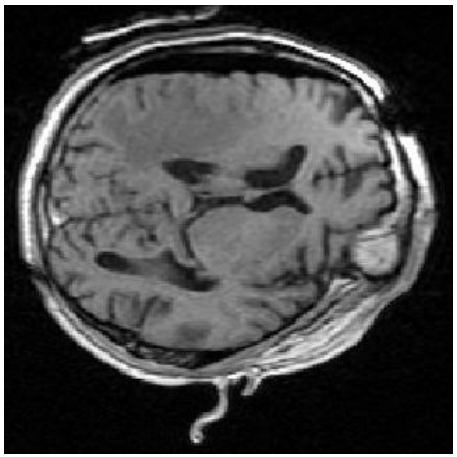

Intra-operative MR T1 weighted image

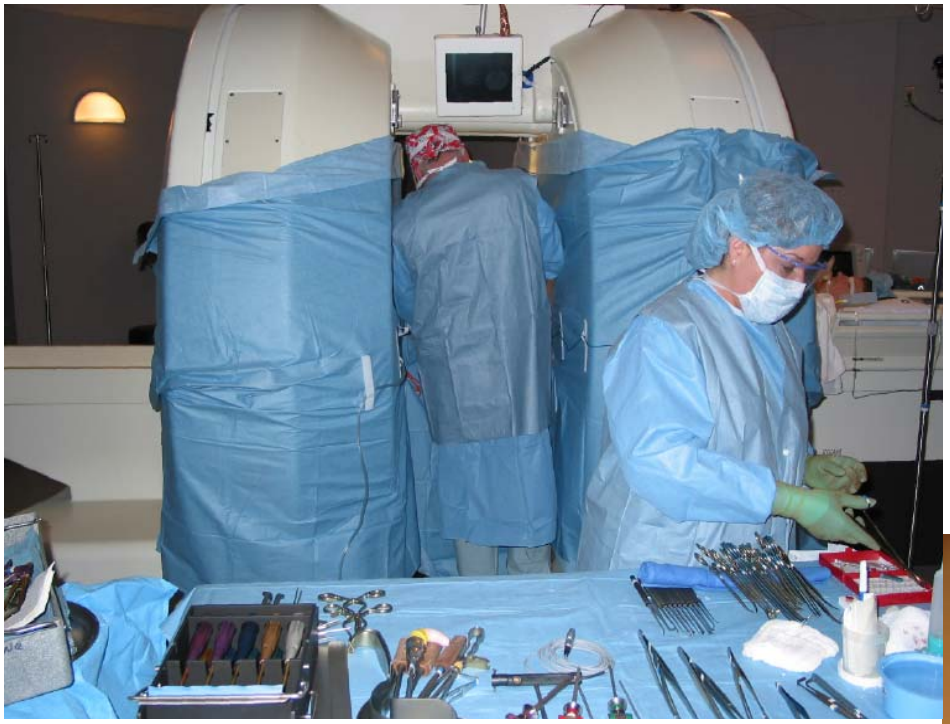

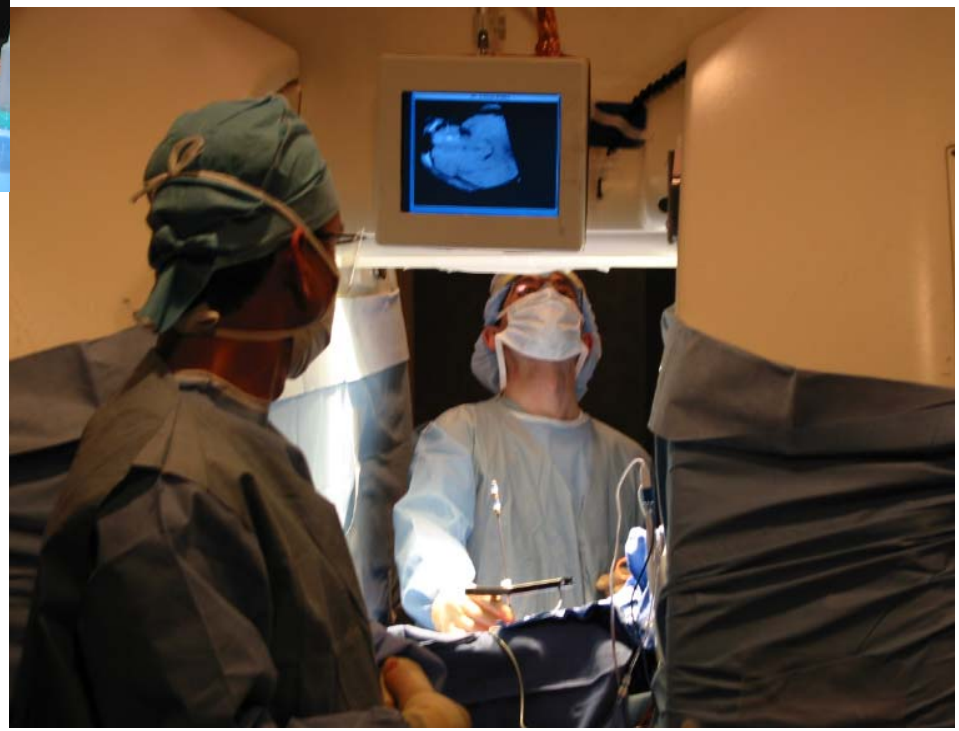

Motivation

- But… intra-operative image have a low magnetic field

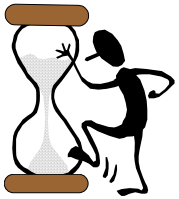

Lower image resolution and higher acquisition time: 256x256x60 T1 MR scan in ~ 4 min.

Not clinically realistic to acquire a full multi sequence data-set during the procedure

Warping the pre-operative data-set to match intra-operative deformation

NON RIGID REGISTRATION

Intraoperative non-rigid registration

- **Fast:** it should not take more than 1 min to make the registration.
- **Robust:** the registration should work with poor quality image, artifacts, tumor...
- **Physics based:** we are not only concerned in the intensity matching, but also interested in recovering the physical (mechanical) deformation of the brain
- **Accurate:** neuro-surgery needs a precise knowledge of the position of the structures

Block matching algorithm

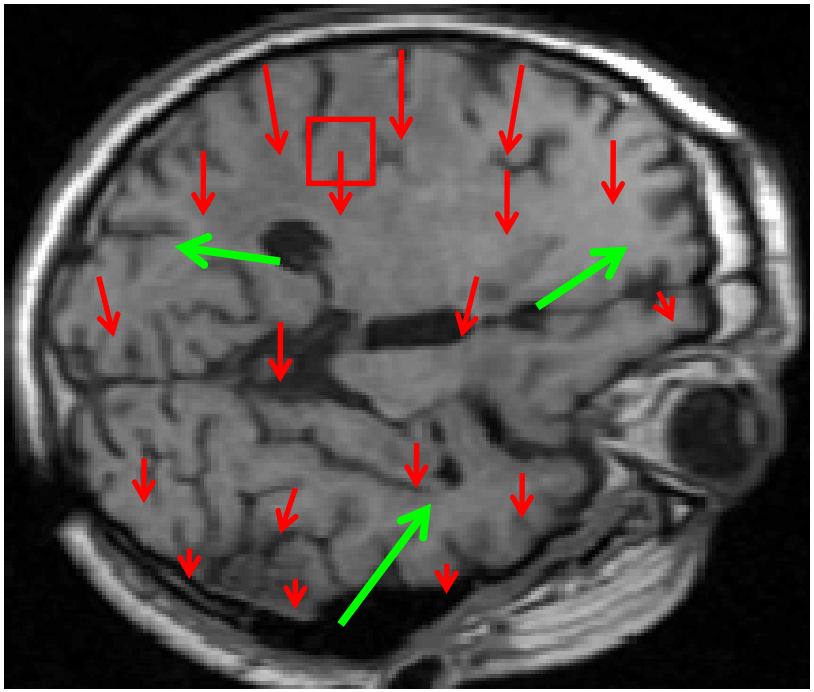

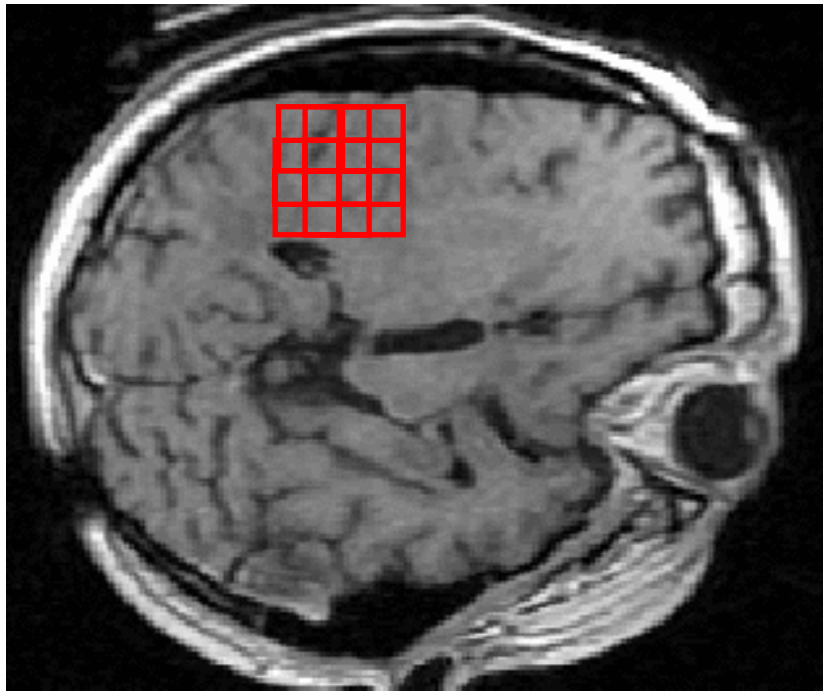

Similarity measure: coefficient of correlation $\in [0:1]$

- Divide a global optimization problem in many simple local ones
- Highly parallelizable

Block matching algorithm

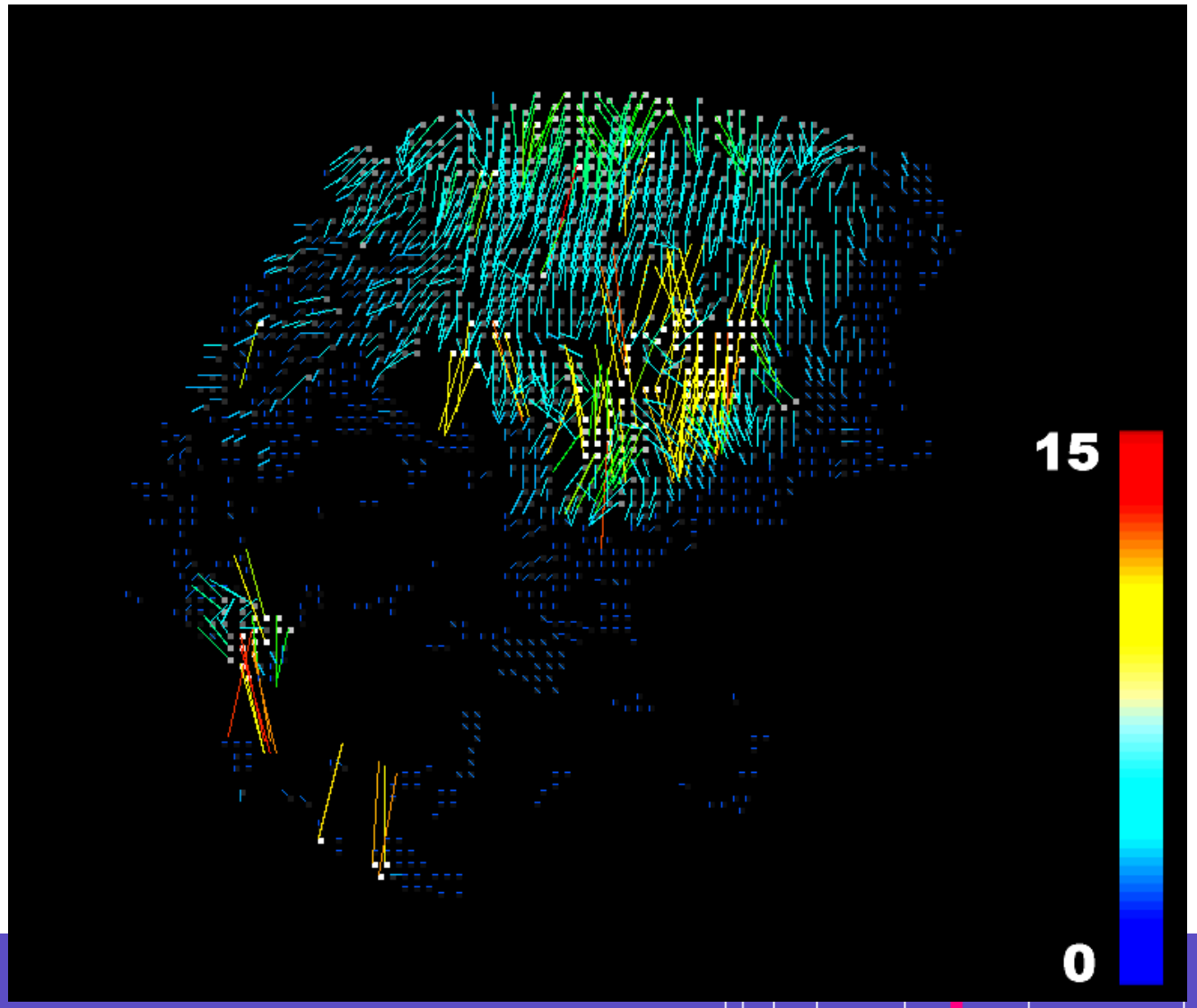

But...
noisy matchings

Patient-specific biomechanical model

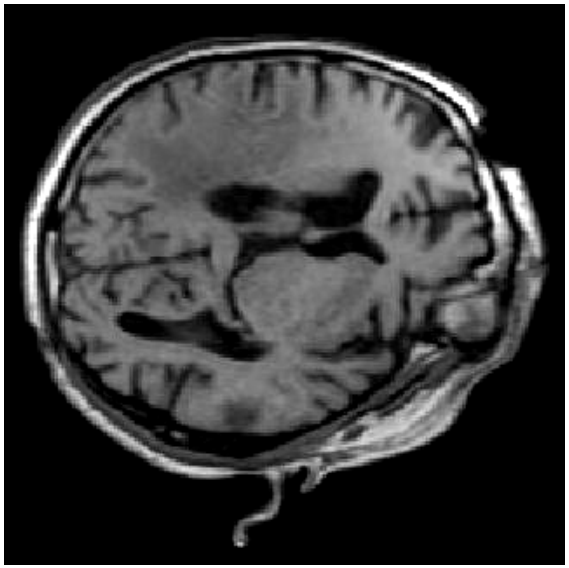

Pre-operative image

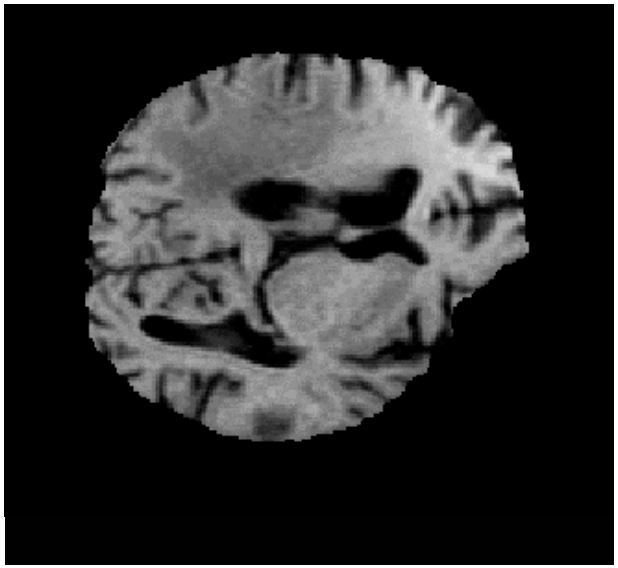

(Semi-) Automatic brain segmentation

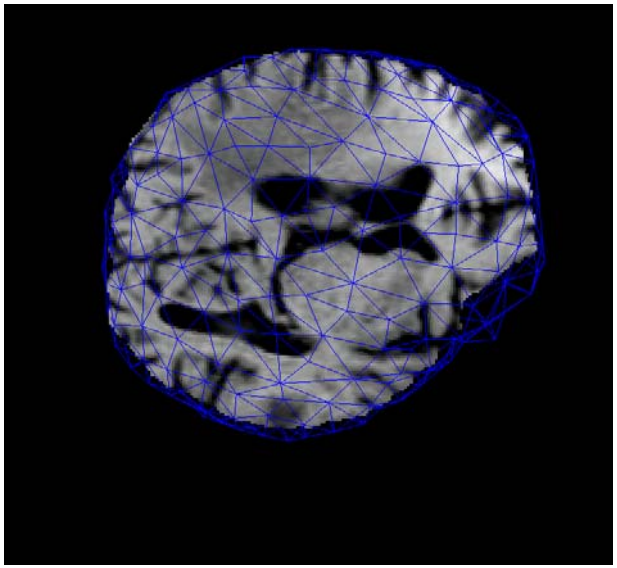

Brain finite element model

Approximation formulation

Trade-off between the mesh mechanical energy and the matching energy :

$$W = \underbrace{U^T K U}_{\text{Mechanical energy}} + \underbrace{(HU - D)^T S (HU - D)}_{\text{Matching energy}}$$

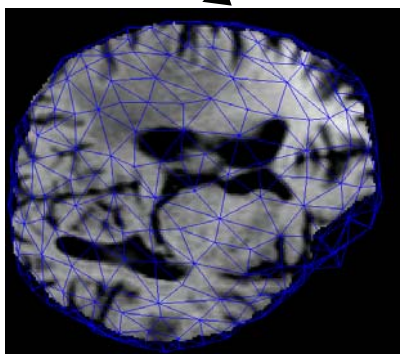

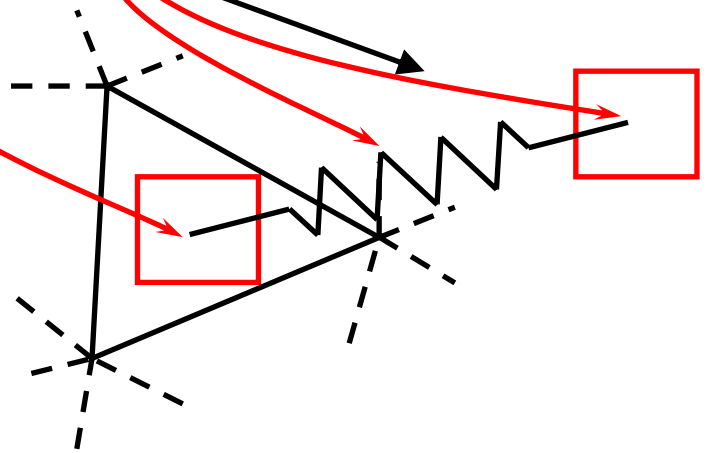

U: Mesh displacement vector (3n)
K: Mesh mechanical stiffness matrix (3n*3n)
H: Interpolation matrix, from the mesh vertices displacements to the block-matching measured displacements (3p*3n)
S: Matching stiffness matrix, including the coefficient of correlation (3p*3p)
D: Measured displacements (3p)

Approximation formulation

$$\frac{\partial W}{\partial U} = 0 \qquad \Rightarrow \qquad \left[K + H^T SH\right] U - H^T SD = 0$$

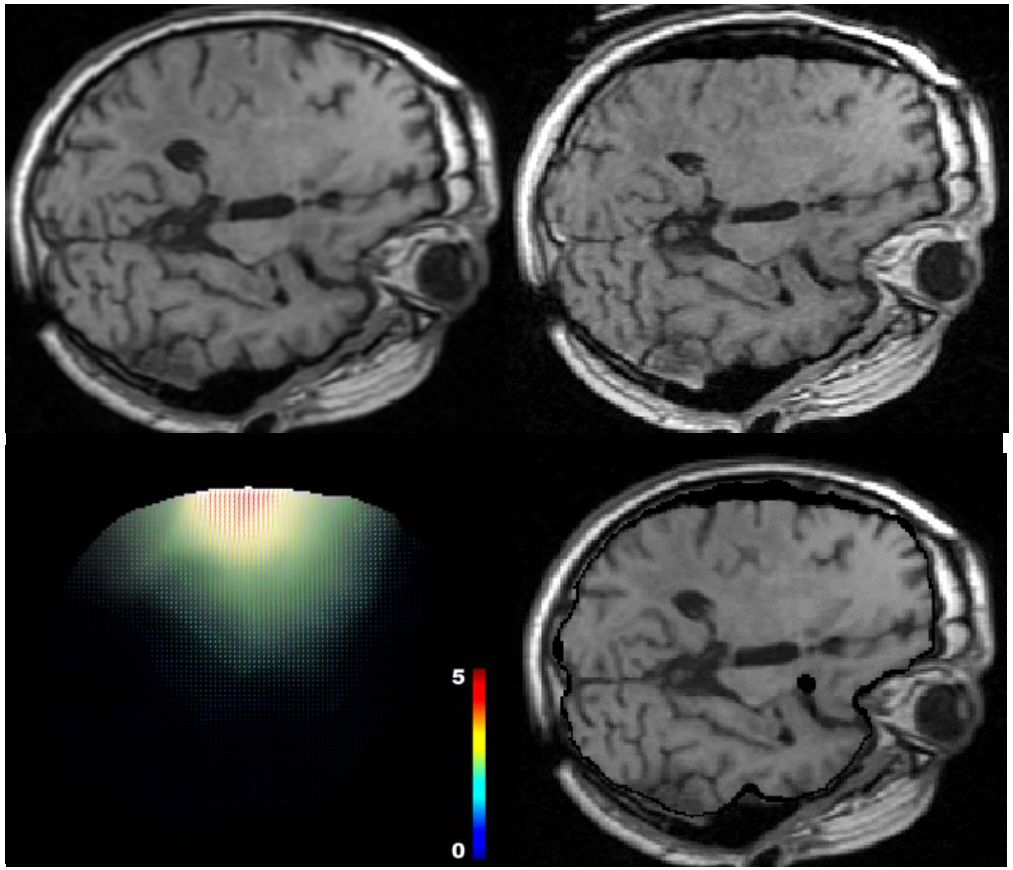

- Realistic displacement field.
- Based on strong mechanical assumptions
- Constant Error

Interpolation formulation

$$W = (HU - D)^T S(HU - D)$$

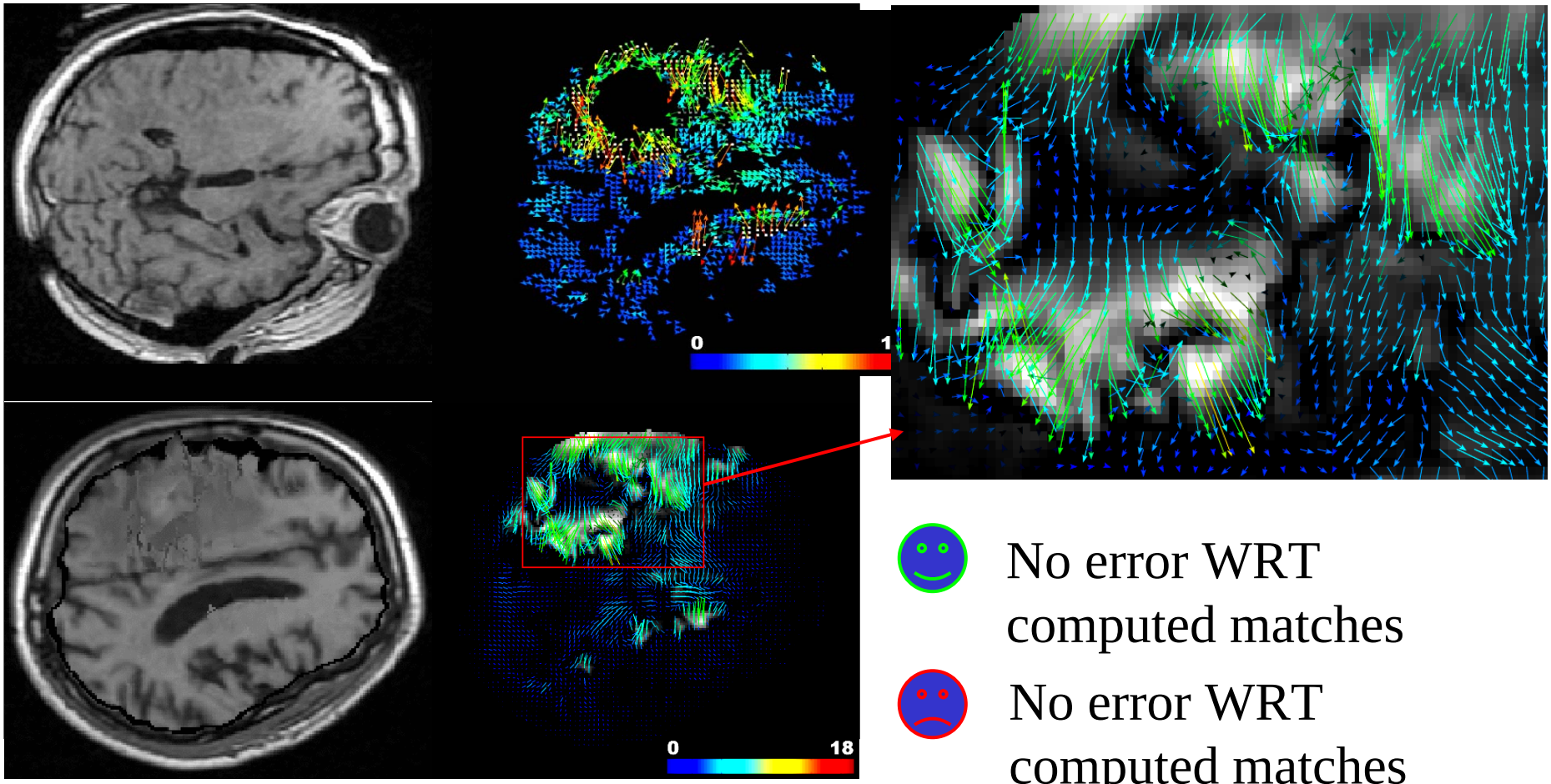

No error WRT computed matches

No error WRT computed matches

Problem Formulation

- Approximation: robust but not accurate
- Interpolation: accurate but not robust

Iterative solving from the approximation to the interpolation:

+ Use the mechanical knowledge introduced by the approximation to select physically realistic matches.

+ Converge to the interpolation while more and more trusting remaining matches

Gradual approach

Method: iterative method introducing an external force F with balance the mesh internal mechanical energy:

$$\left[K + H^T S H\right] U = H^T S D + F$$

$$W = U^T K U + (HU - D)^T S (HU - D)$$

Algorithm:

$$F_i \Leftarrow K U_i$$

$$U_{i+1} \Leftarrow \left[K + H^T S H\right]^{-1} \left[H^T S D + F_i\right]$$

At each iteration, reject % of outliers based on a least trimmed squared algorithm.

Gradual approach

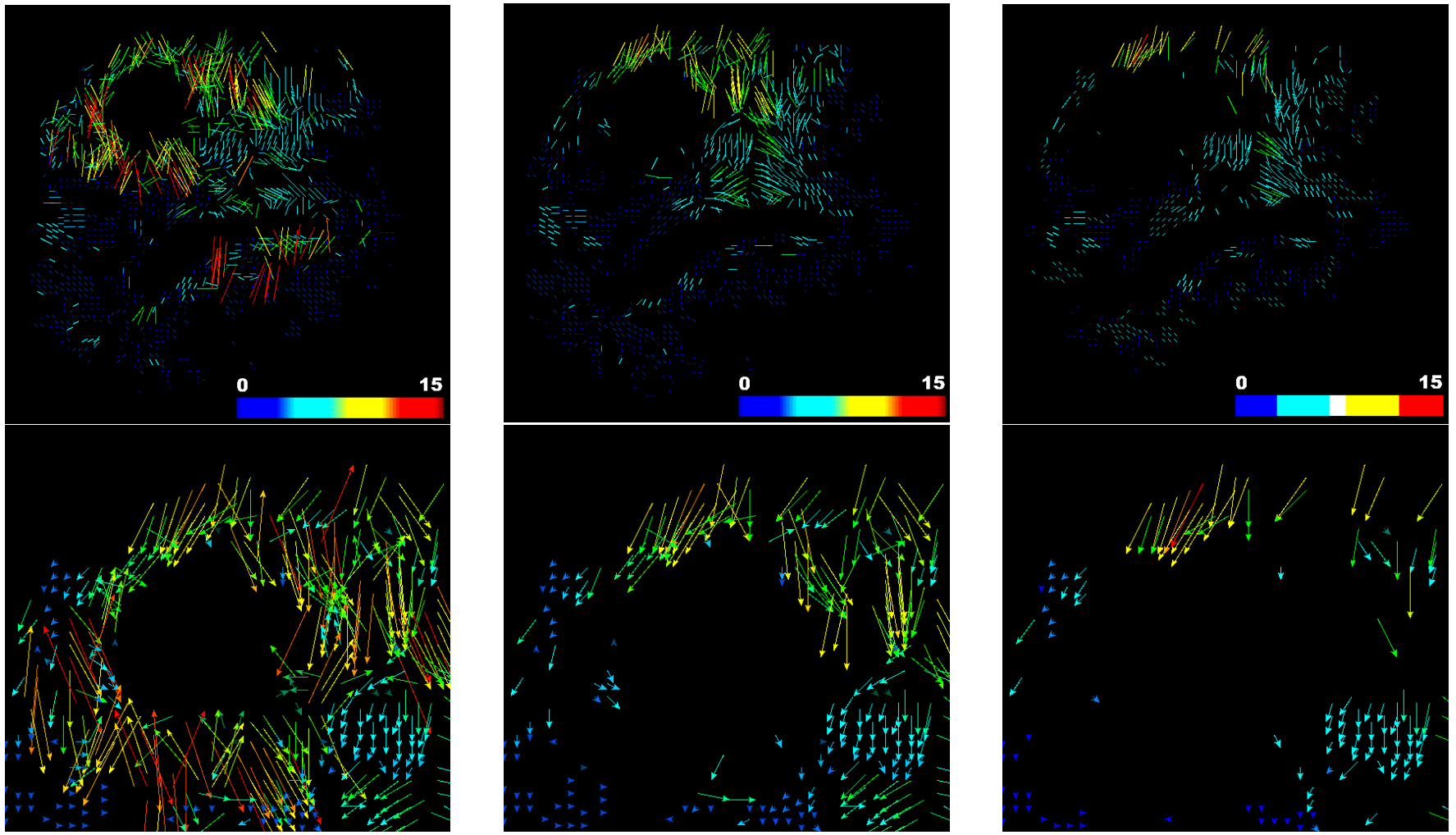

First step | After 5 steps | After 10 steps

Matching stiffness ?

- Aperture problem:

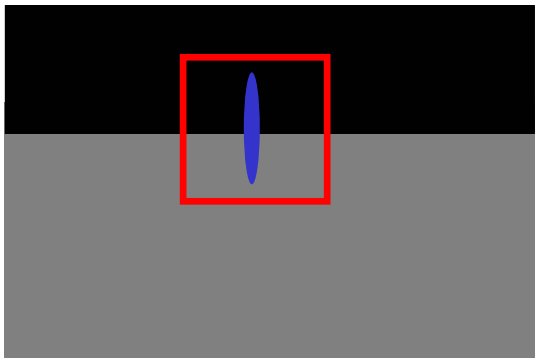

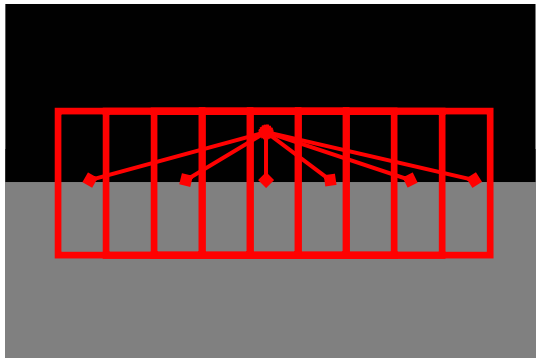

- Use of the local structure tensor to weight the matching stiffness

$$T = \frac{G * \nabla I \nabla I^T}{trace(G * \nabla I \nabla I^T)}$$

Anisotropic ponderation

$$\underbrace{(HU - D)\,S\,(HU - D)^T}_{\text{Matching energy}}$$

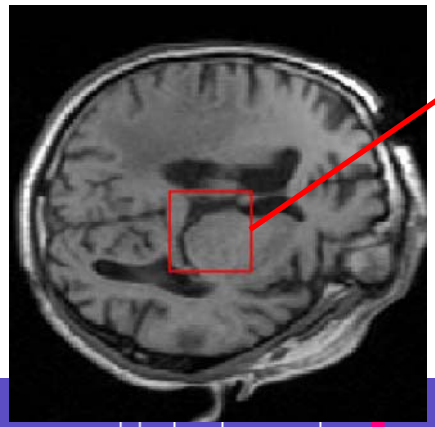

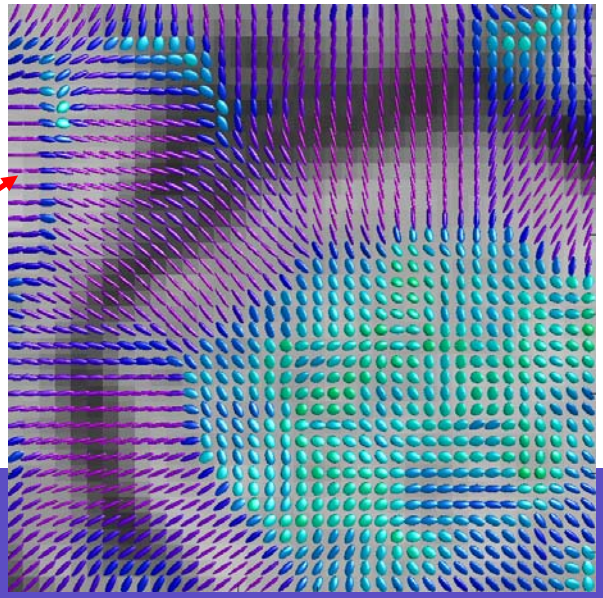

Results

- Tested on 6 (extreme) cases
- Parallel version runs in 35 seconds on a 10 dual 2GHz PC cluster
  - 7x7x7 block size
  - 11x11x25 window
  - 1x1x1 step
  - 50 000 blocks
  - 10 000 tetrahedra
- 60 landmarks:
  - Average error = 0.75mm
  - Maximum error = 2.5mm

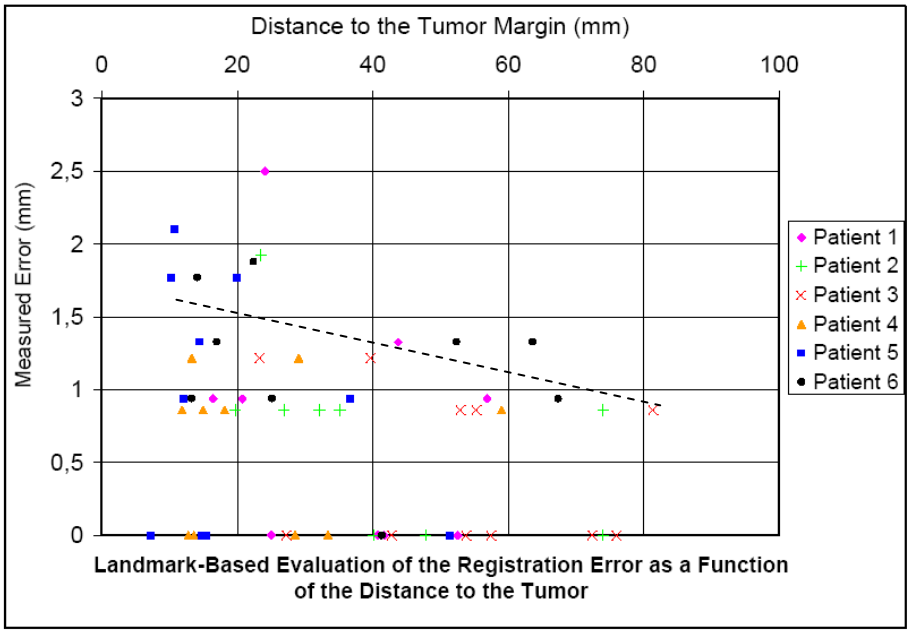

Max displacement (mm)	13.18
Average displ ± std. dev. (mm)	3.77 ± 3.3
Average error± std. dev. (mm)	0.75 ± 0.6
Max. error. (mm)	2.50
Average relative error (%)	20

Results

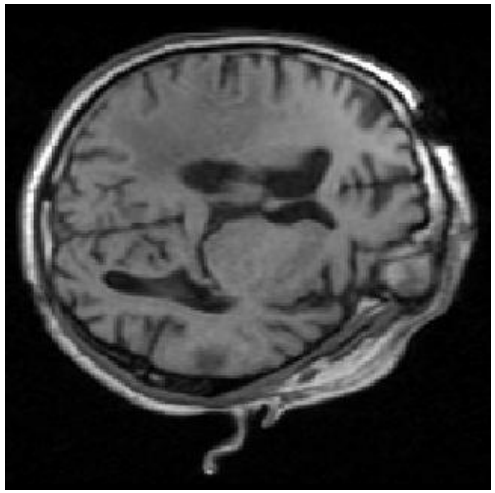
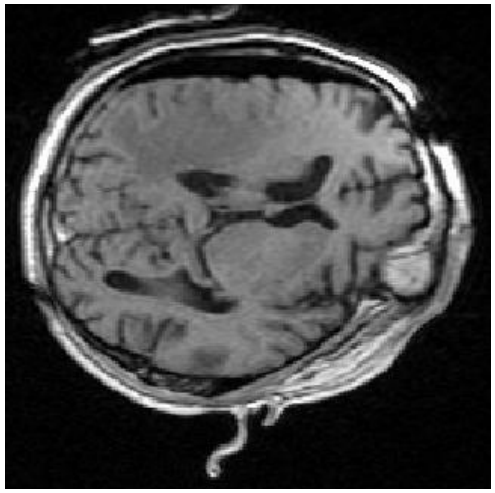
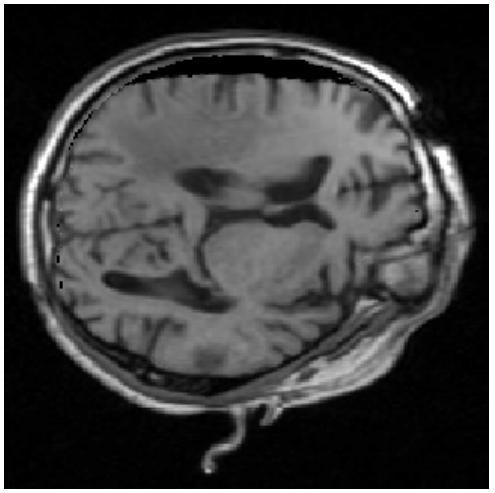
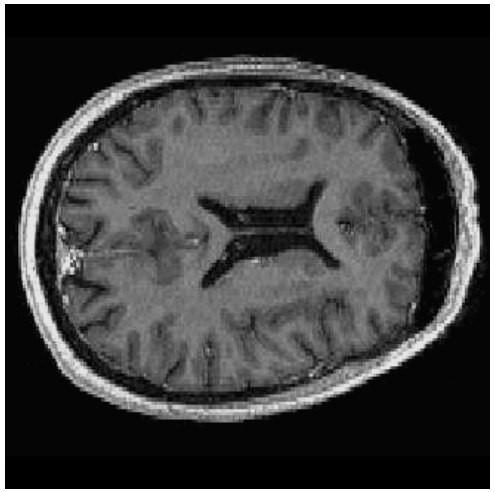
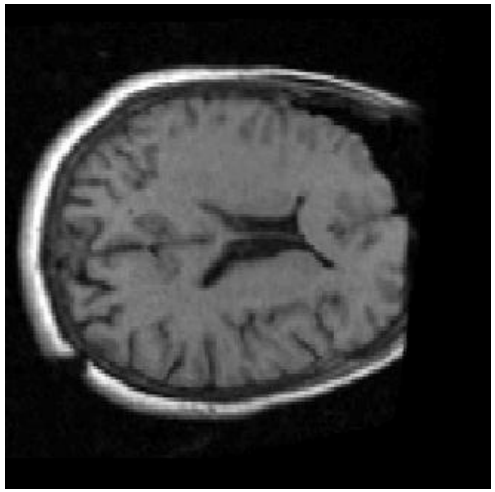
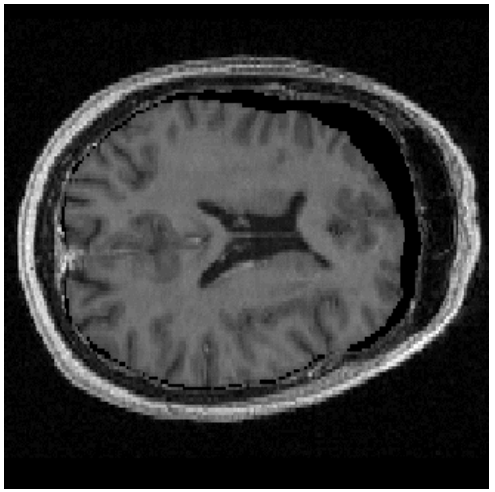

Pre-operative

Intra-operative

Registered pre-operative

Results

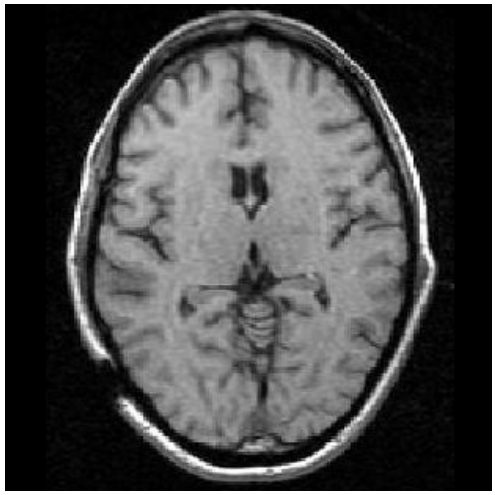
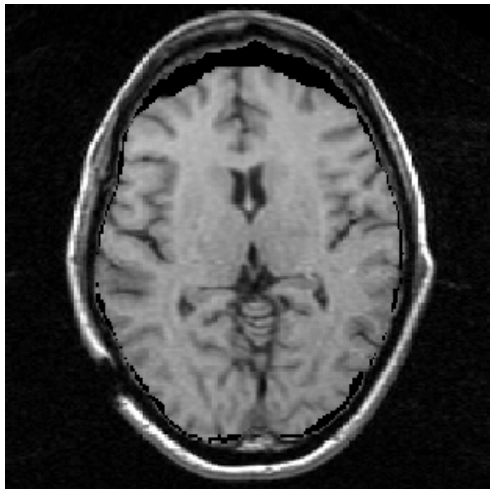
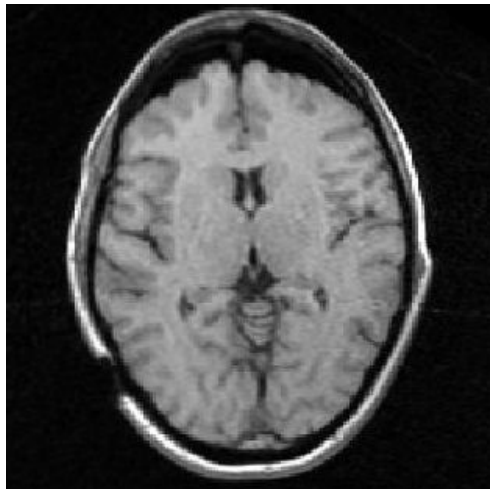
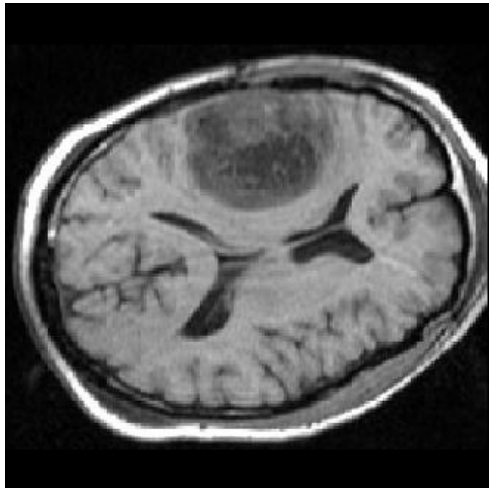
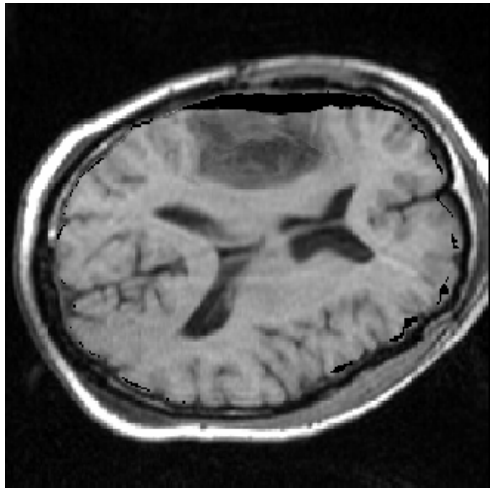
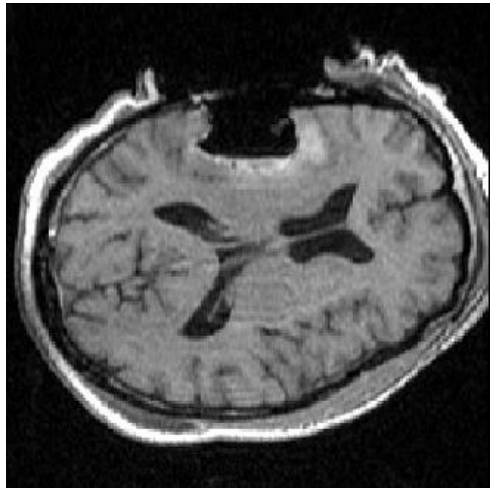

Pre-operative

Registered pre-operative

Intra-operative

Results

Image guided therapy

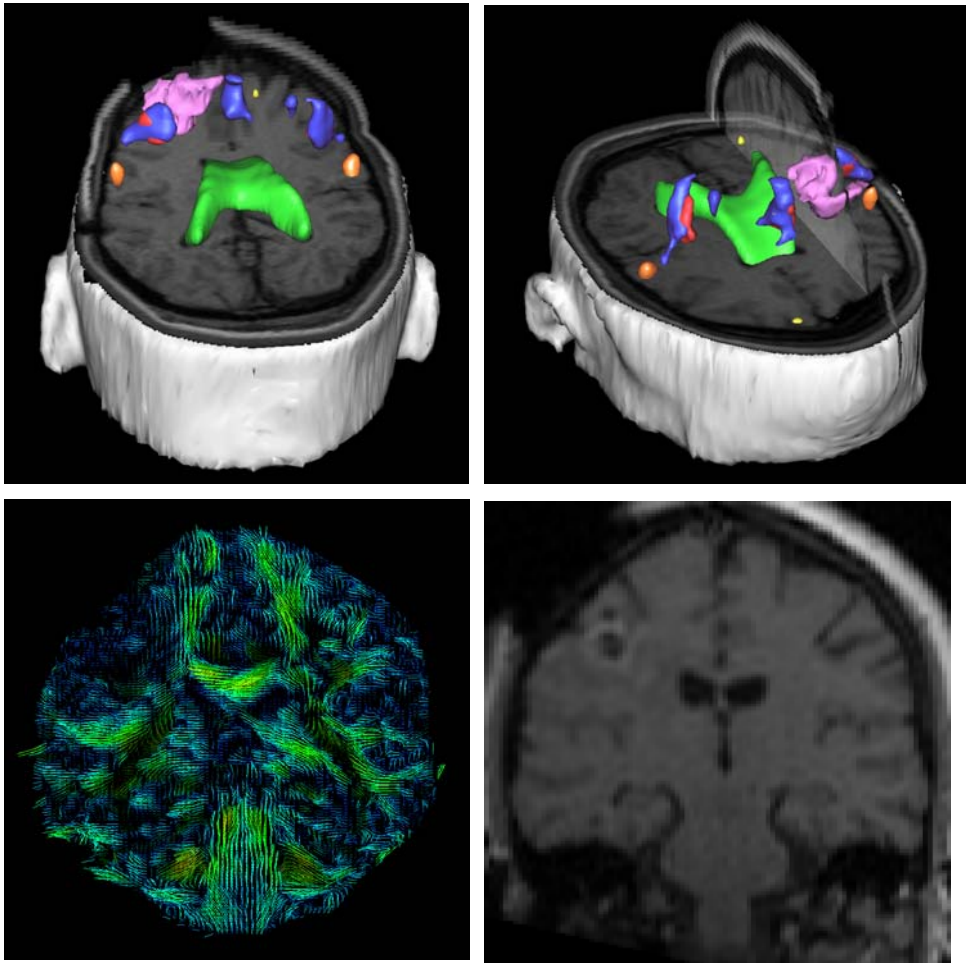

- fMRI data (activation map)
- DT MRI

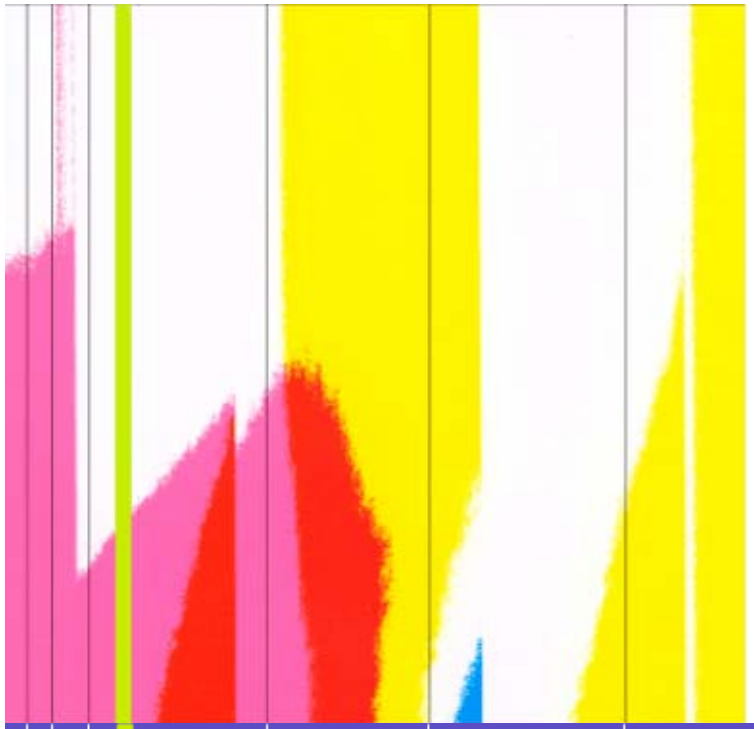

Brain Tumor Growth Modeling

INSTITUT NATIONAL
DE RECHERCHE
EN INFORMATIQUE
ET EN AUTOMATIQUE

INRIA
SOPHIA ANTIPOLIS

Problem position

- Understanding both the mechanical influence and the diffusion process of gliomas
- Using the model for
  - Identify invaded area that are not visible in the MRI
  - Predict future evolution of the tumor
  - Characterize the tumor

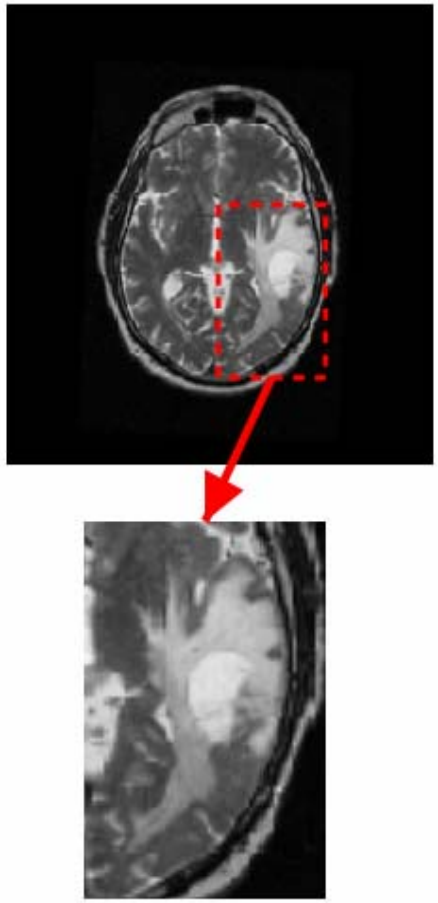

Tumor biology

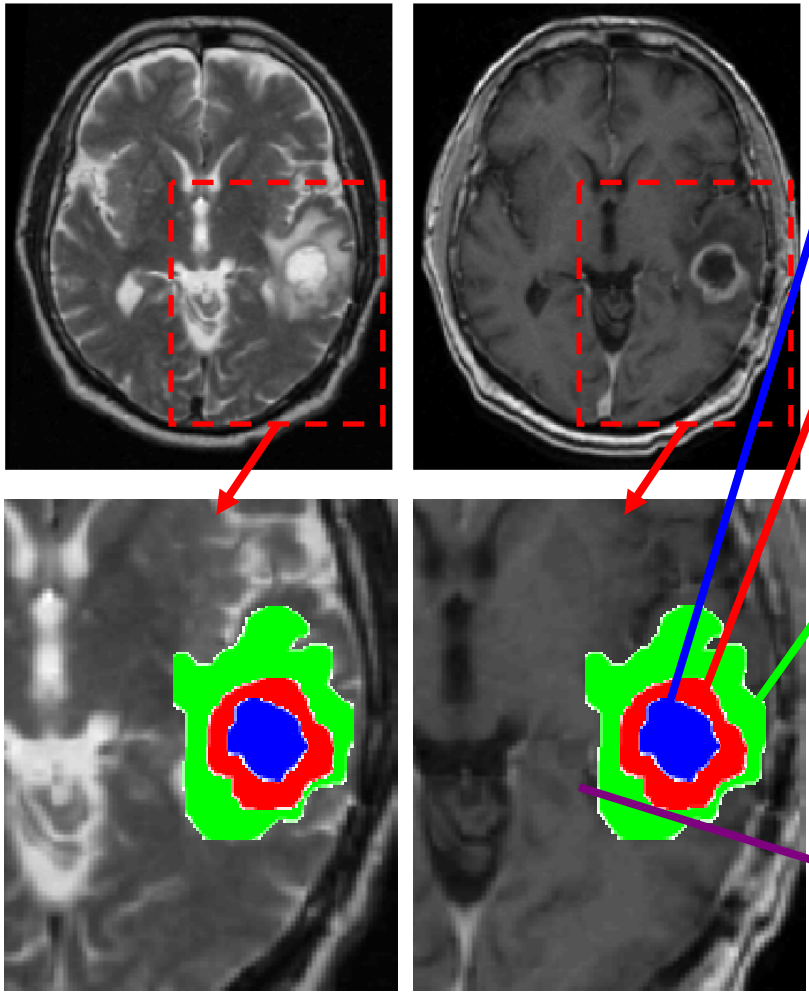

T2 MRI T1 MRI + gad

Necrotic center

Active tumor cells
+ angiogenesis

Edema and
infiltrating tumor
cells

Mass effect

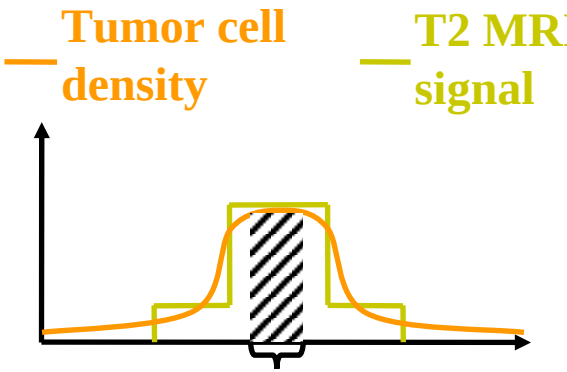

Nécrosis

Observability !

Geometric model

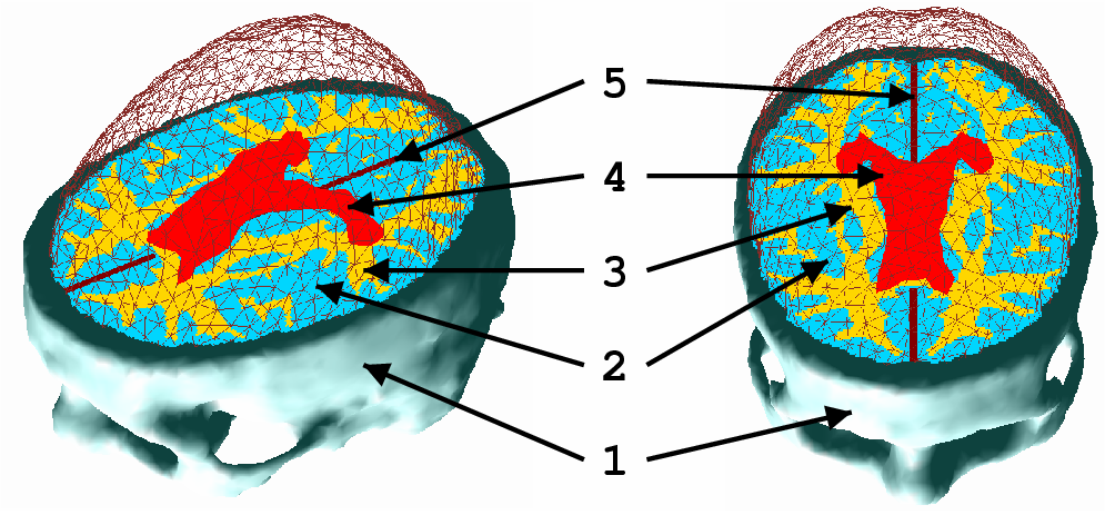

1. Skull.
2. Gray matter
3. White Matter
4. Ventricles
5. Falx cerebri

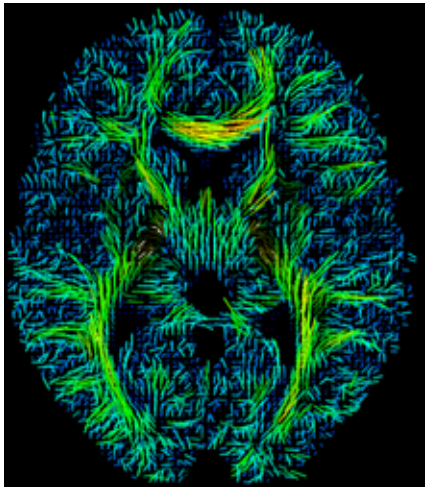

DTI (atlas)

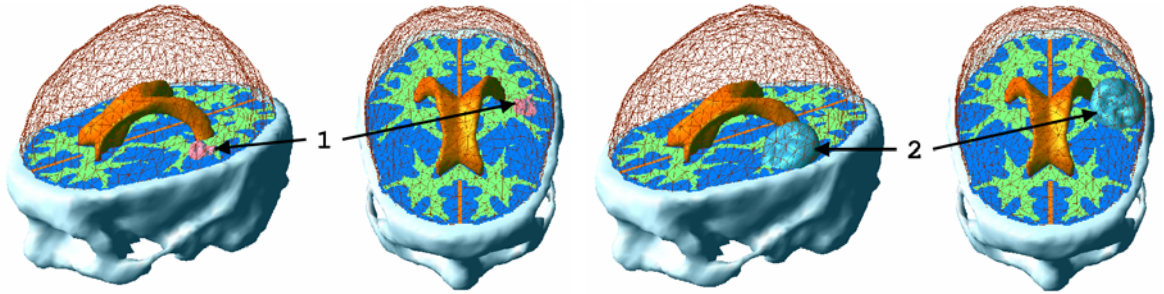

Initial position of the tumor

Mecanical model

- Linear elasticity for the brain :

$$\sigma = \lambda\, tr(\varepsilon) + 2\mu\,\varepsilon \quad \varepsilon = \frac{1}{2}\left(\nabla u + \nabla u^T\right)$$

σ = Stress
ε = Stress

λ, μ = Lamé Coefficient
u = Displacement

- Influence of tumor cells on the mechanics

$$\mathrm{div}(\sigma - \alpha c\, I_3) + Fe = 0$$

α = Coupling factor
Fe = External forces

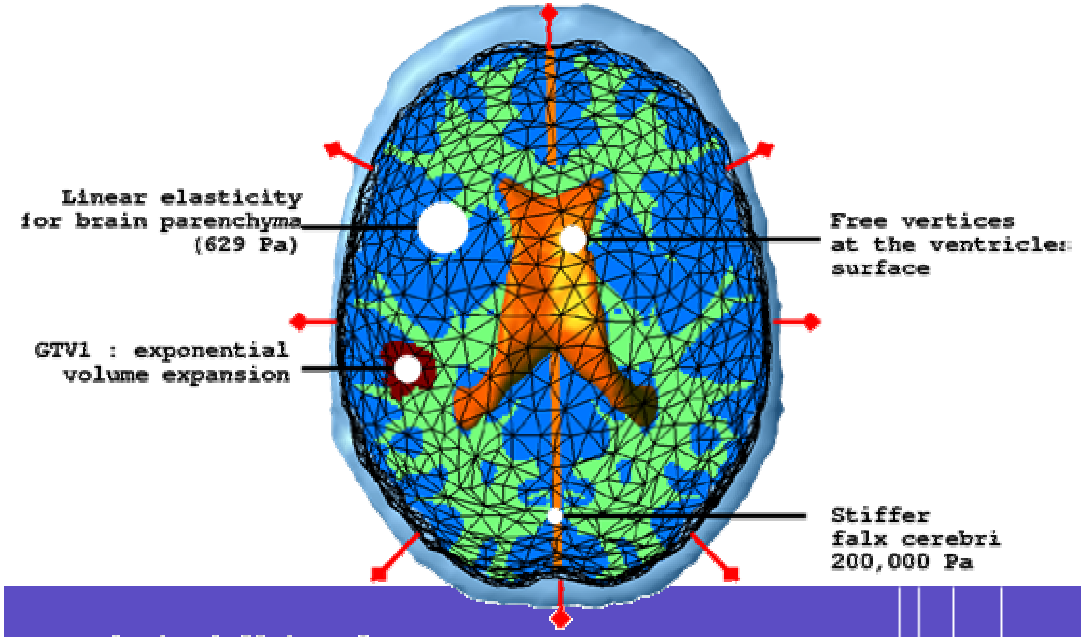

Summary:

- *Linear relationship force | displacement*
- *Tumor acts as a local pressure*

INRIA SOPHIA ANTIPOLIS

Diffusion model

Reaction diffusion equation

$$\frac{\partial c}{\partial t} = \nabla.(D\nabla c) + \rho c(1-c)$$

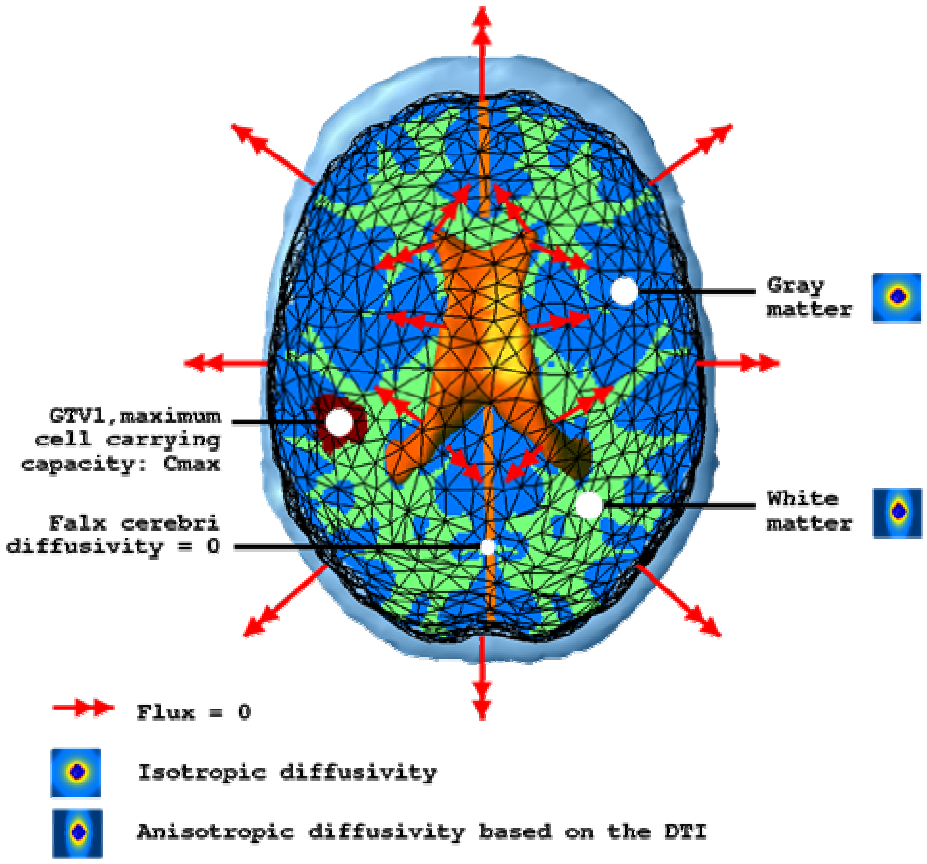

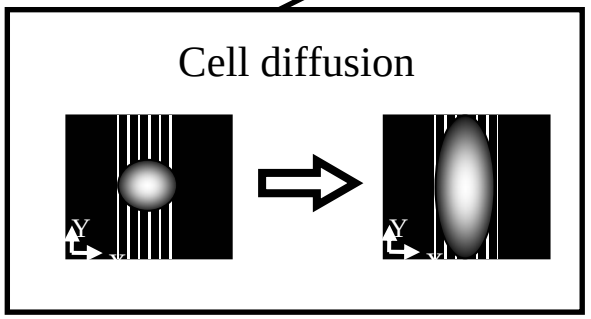

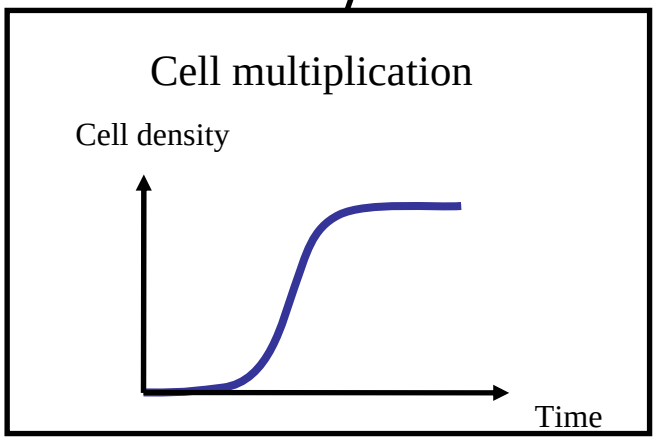

Tumor Growth simulation

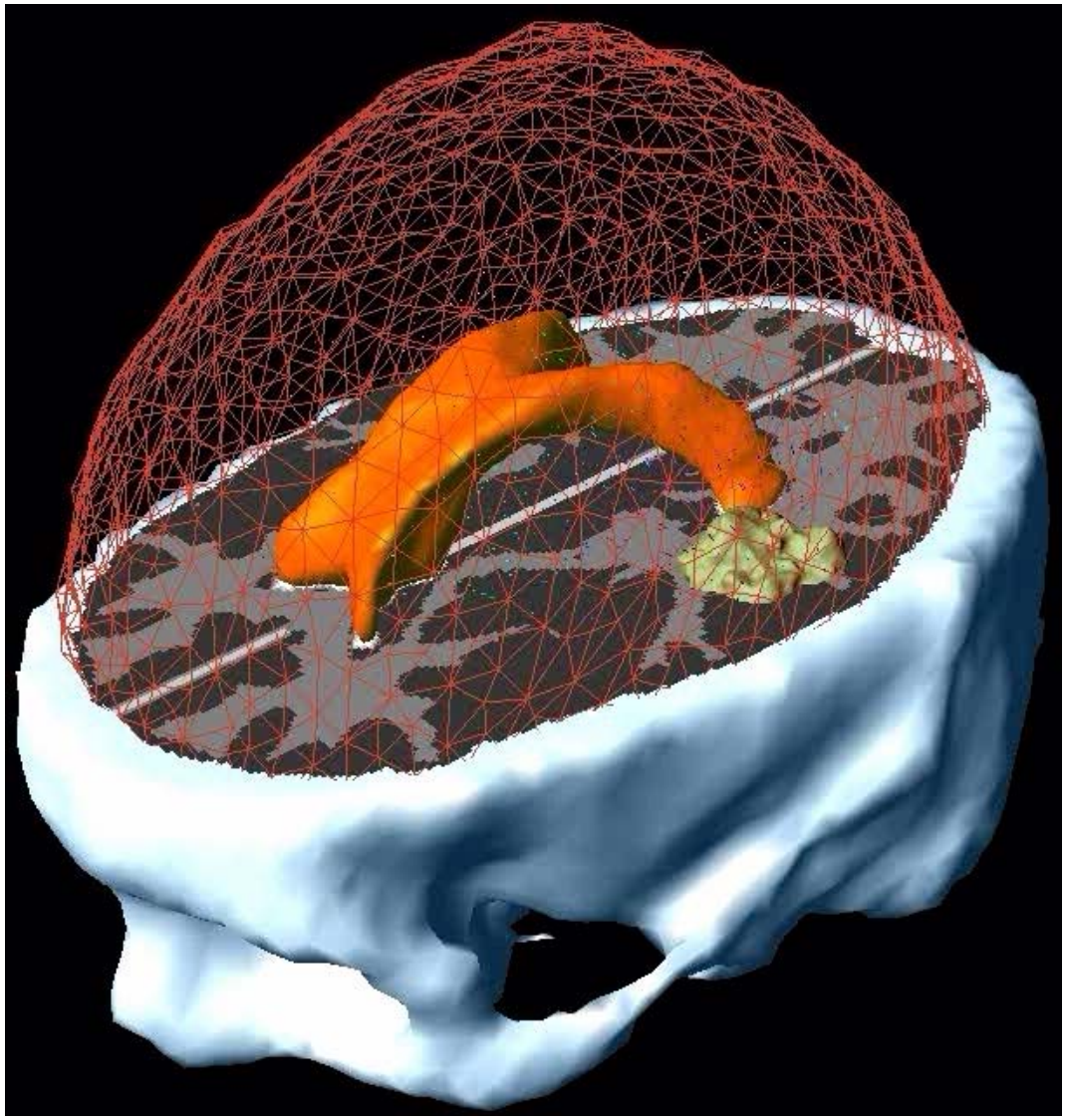

Results

March 2002

March 2002 + initial contour

September 2002

September 2002 + simulation contours

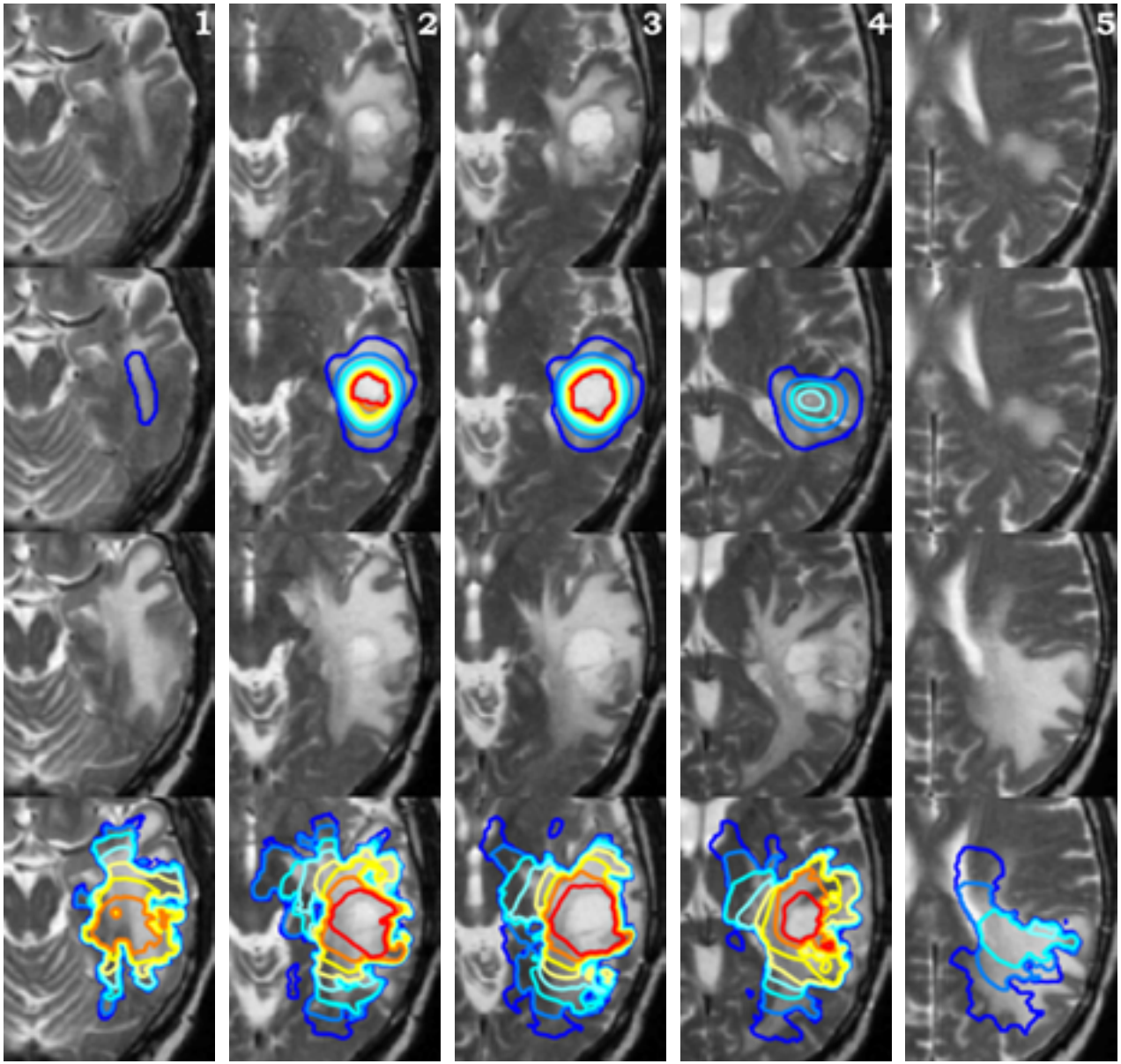

Analyzing Diffusion Model

$$\frac{\partial c}{\partial t} = \nabla.\left(D\nabla c\right) + \rho c(1-c)$$

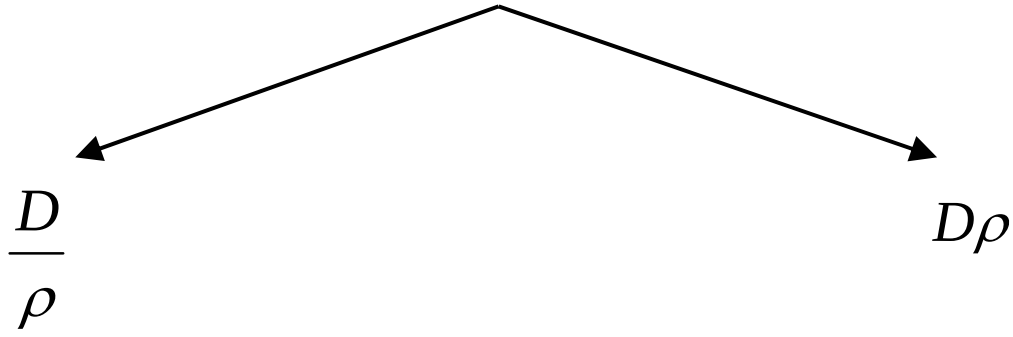

- Tumor profile
- Infiltration extent
- Extrapolation
- Not observable from images

- Growth speed
- Parameter Estimation
- Quantification
- Observable from time series of images

Model Based Growth Quantification

t_1

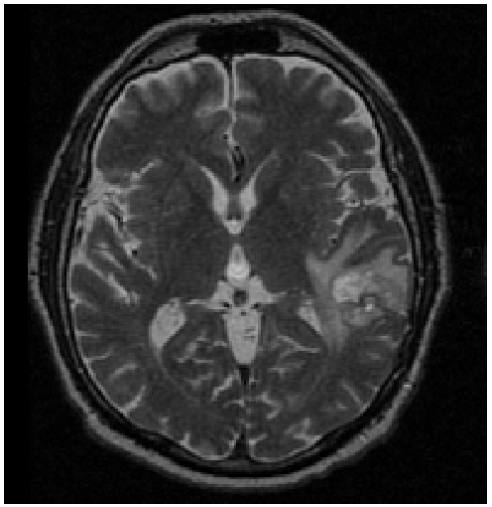

6 months

$[D\rho]_{wm}, [D\rho]_{gm}$?

t_2

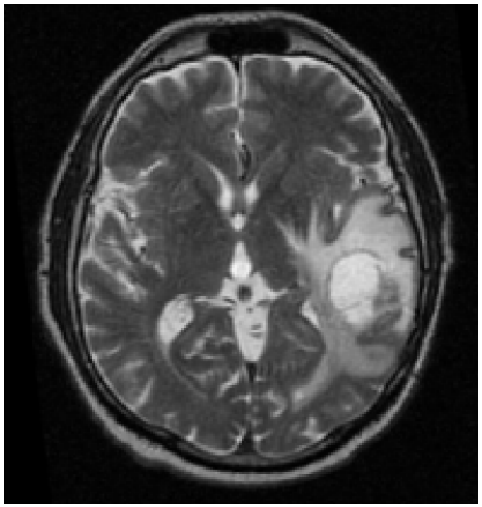

- Observables:
  - Tumor fronts (CTV extent) :
    - Tumor infiltrated edema extent for high grade tumors
    - Bulk tumor extent for low grade tumors
  - White matter segmentation and DTI.
- Only $D\rho$ is observable from the images.
- What are growth speeds in the white matter and in the grey matter?

Front Motion Approximation

• Again using the asymptotic traveling wave solution.

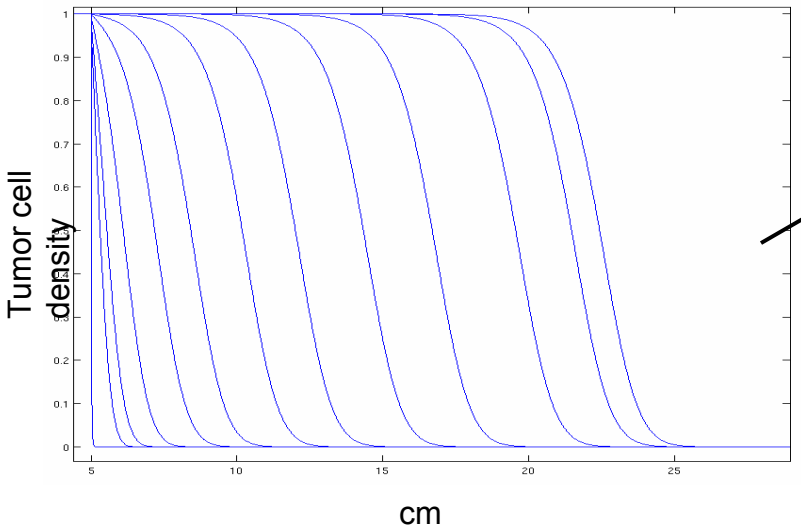

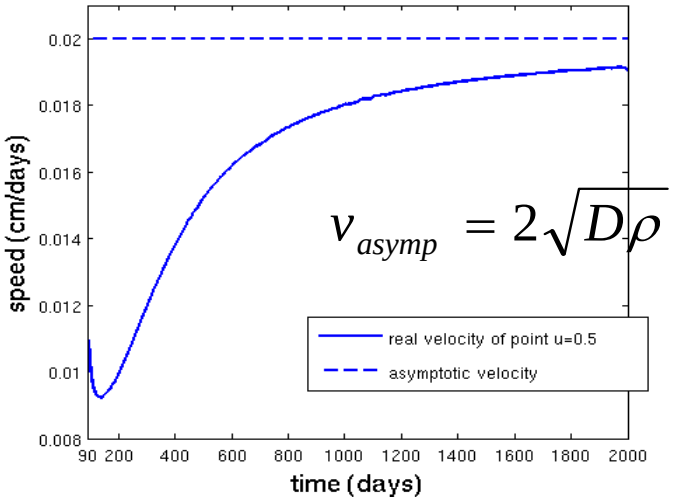

• Assuming visible tumor front is an iso-density surface.

• Traveling time formulation for the motion of the tumor front gives:

$$\sqrt{\nabla T' D \nabla T} = \frac{1}{2\sqrt{\rho}}$$

Recursive Fast Marching

- Anisotropic Eikonal equation
- Recursively correcting errors due to anisotropy.

$$\sqrt{\nabla T' D \nabla T} = \frac{1}{2\sqrt{\rho}}$$

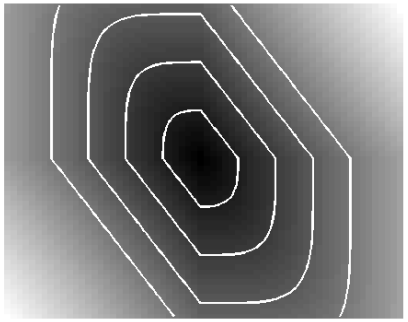

Normal Fast Marching

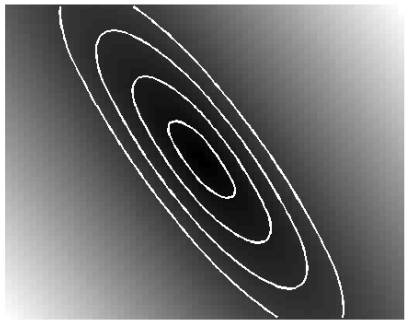

Recursive Fast Marching

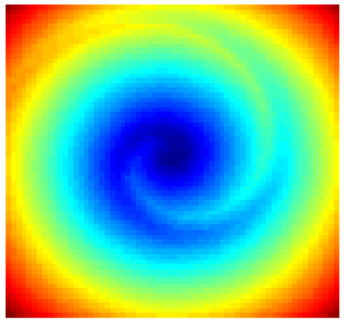

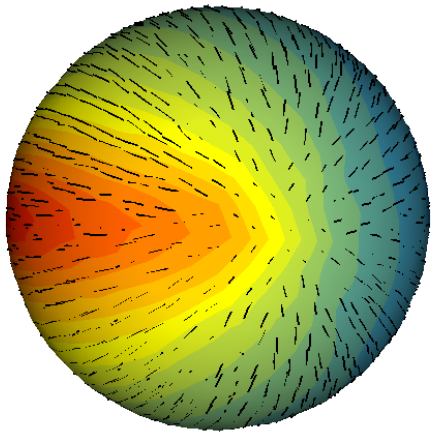

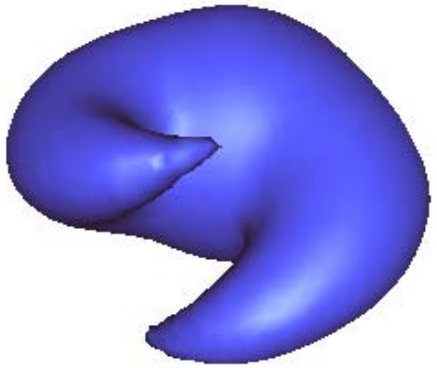

- Fast and efficient even for very high anisotropies.
- Works on general meshes.

Identifying Parameters

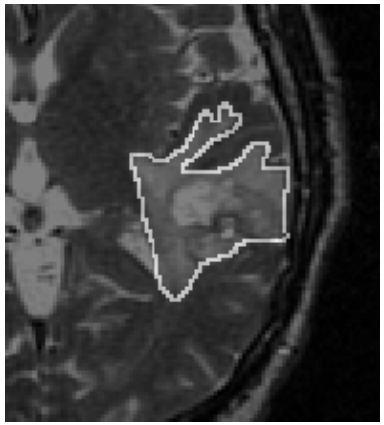

Γ_1

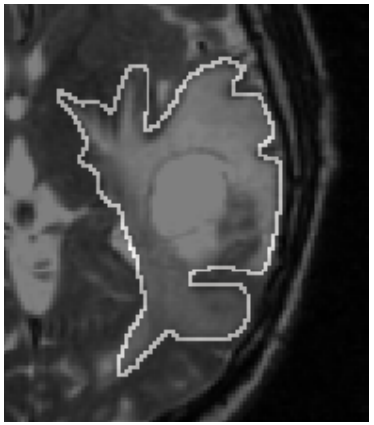

Γ_2

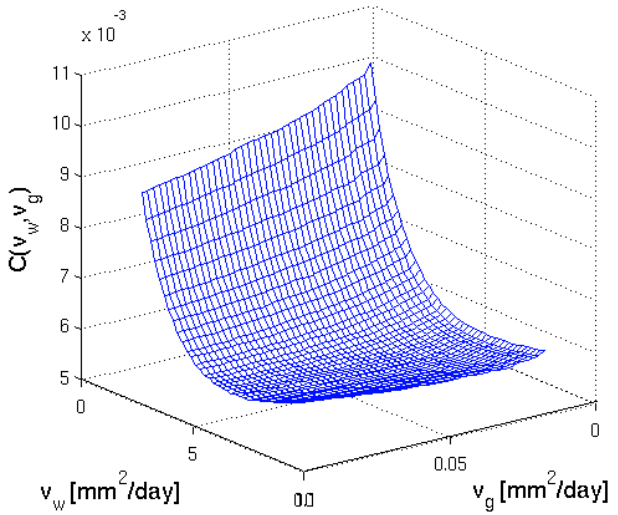

$$C(v_w, v_g) = \frac{1}{2}\left[dist\left(\Gamma_2, \overline{\Gamma_2}\right), dist\left(\overline{\Gamma_2}, \Gamma_2\right)\right]$$

$$\overline{\Gamma_2} = \left\{ \begin{array}{l} x \middle| T(x) = t_2 - t_1, \\ \sqrt{\nabla T' D \nabla T} = \dfrac{1}{2\sqrt{\rho}}, T(\Gamma_1) = 0 \end{array} \right\}$$

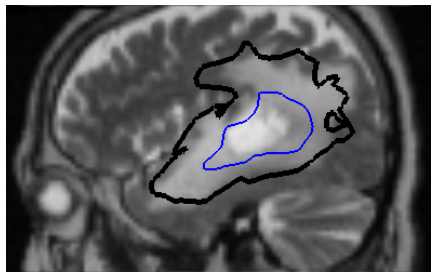

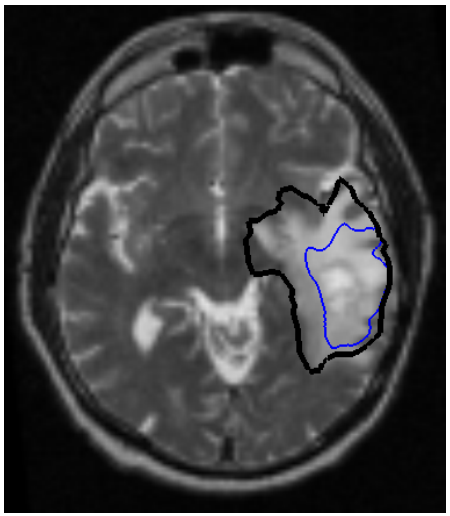

$$[D\rho]_{wm} = 4.7 \times 10^{-2} \frac{mm^2}{day}$$

$$[D\rho]_{gm} = 4.3 \times 10^{-4} \frac{mm^2}{day}$$

Extrapolating Tumor Invasion

- CT and MR have limited resolution for tumor cells.
- We do not see the whole tumor infiltration.
- Use of growth dynamics to understand the extents of the tumor.

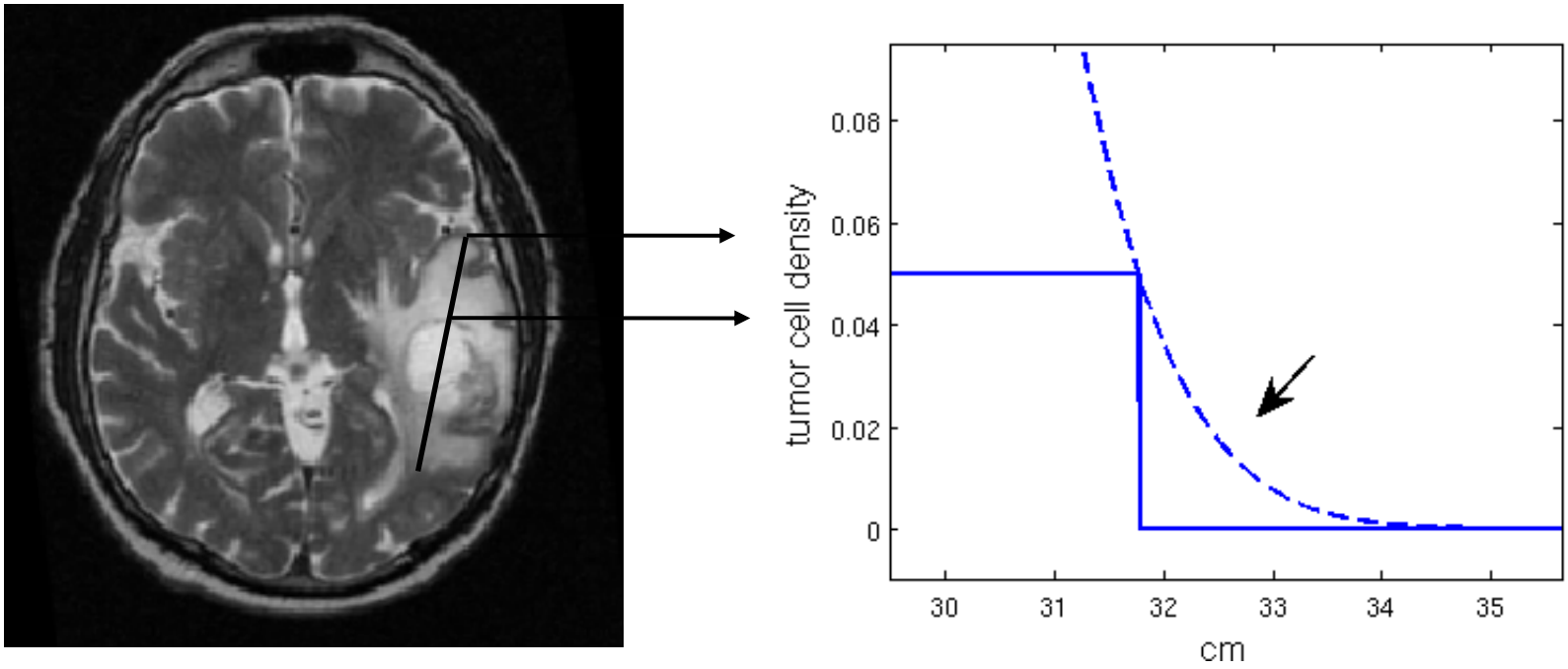

Tail Distribution

$$\frac{\partial c}{\partial t} = \nabla.(D\nabla c) + \rho c(1-c)$$

Traveling wave solution in the infinite cylinder with constant D:

$$c(\vec{x},t) = u(\vec{x}\cdot\vec{n} - vt) = c(\bar{\xi})$$

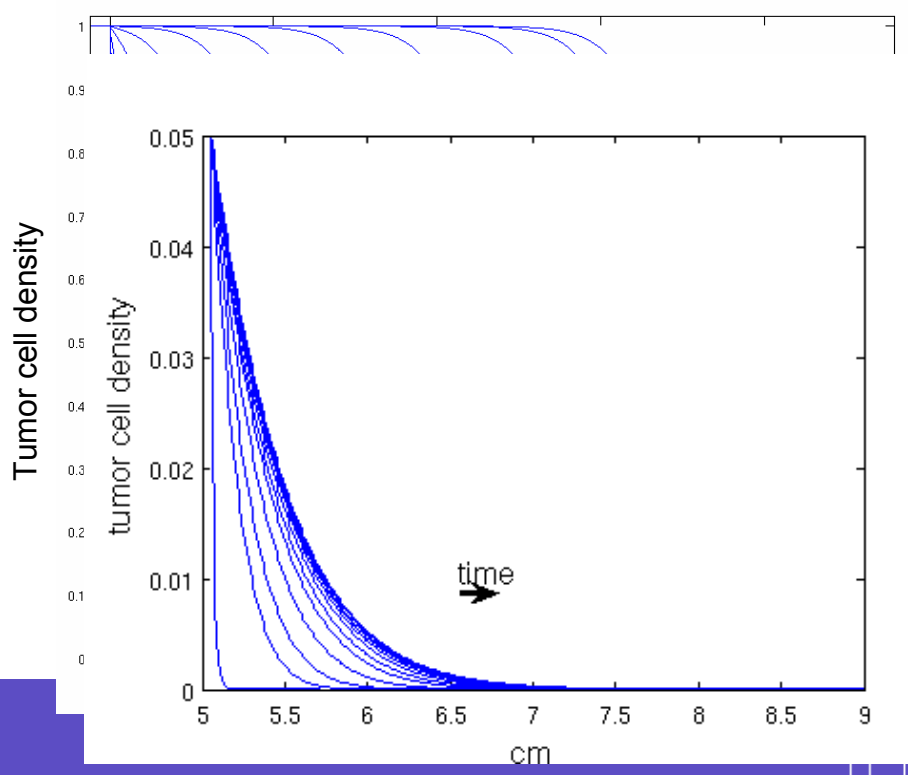

$$u(\xi) = u_0 \exp\left(-\sqrt{\frac{\rho}{\vec{n}\cdot(D\vec{n})}}\xi\right)$$

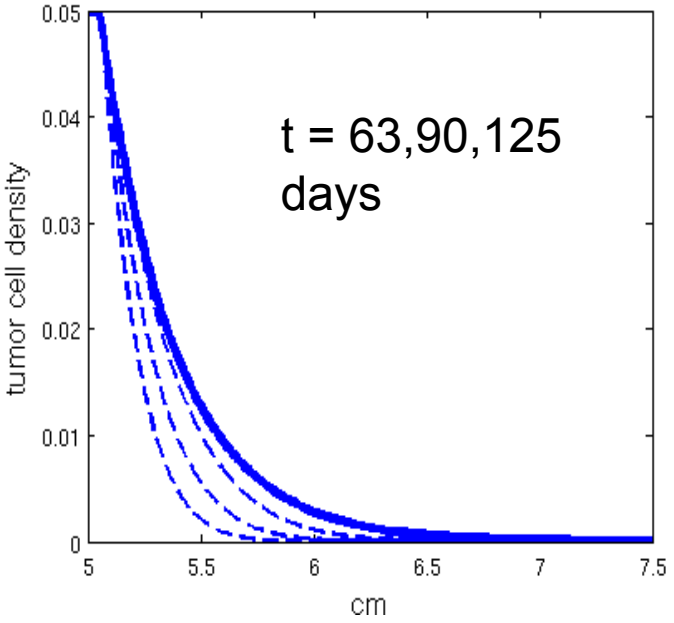

$$\frac{\sqrt{\nabla u\cdot(D\nabla u)}}{\sqrt{\rho u}} = 1$$

Comparison with the Model

From 5% to 1% - Using same parameters

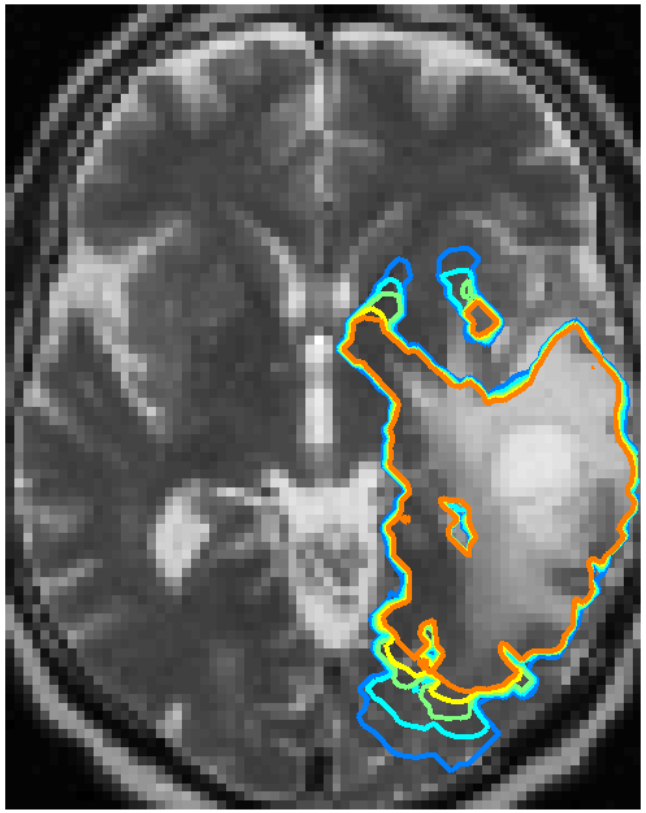

After 6 months
according to the model

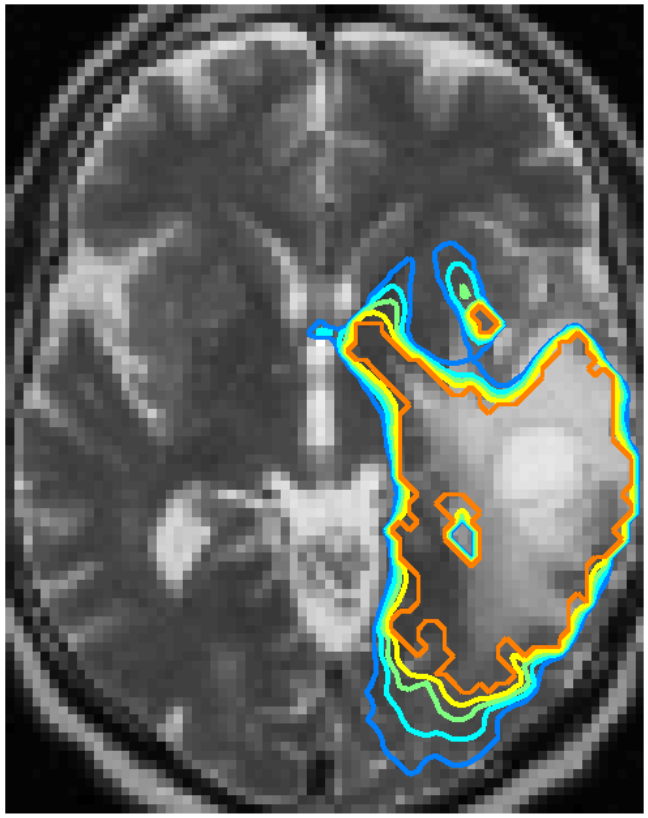

Approximated tails

Invasion Extent vs. Irradiation Margin

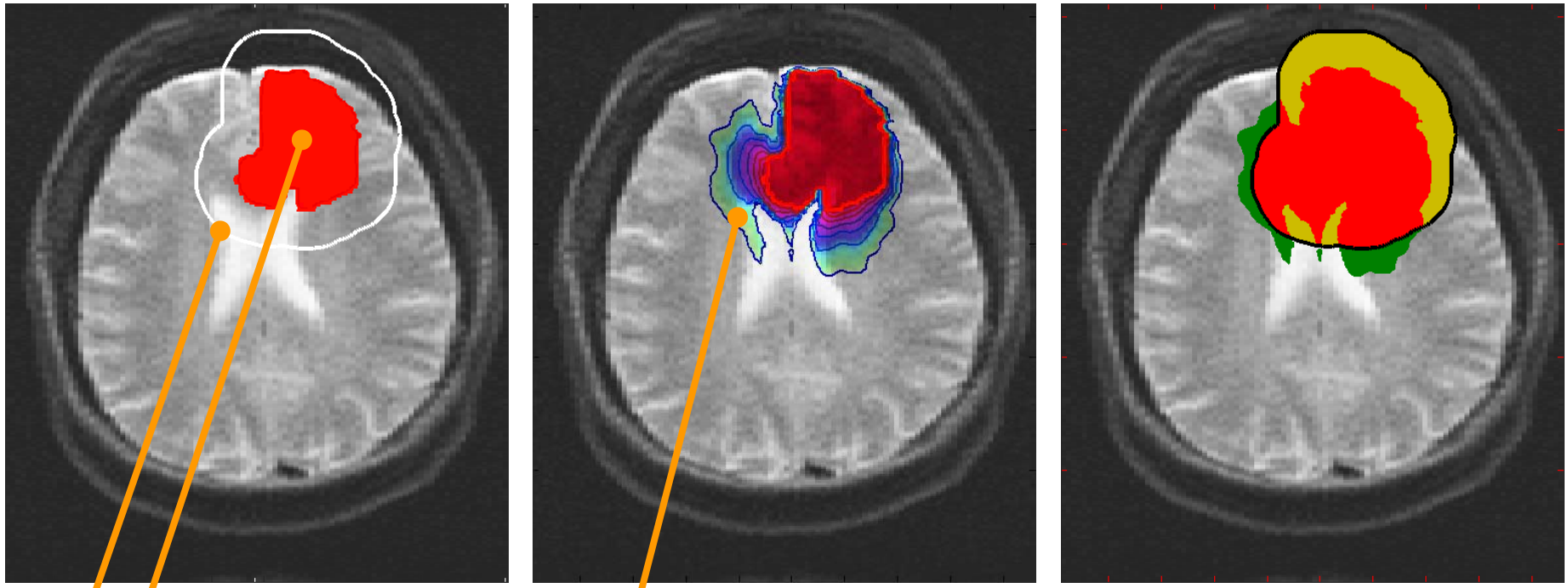

Visible tumor

Radiotherapy margin

Simulated probability of finding tumor cells

Invaded area targetted by radiotherapy

Area targetted by radiotherapy BUT NOT invaded

Area invaded BUT NOT targetted by radiotherapy

Perspectives I

- Validation of the model through
  - Predicting growth for untreated cases.
  - Recurrence after surgery/therapy.
- Provide a confidence interval
  - In the extent of the tumor
  - In the tumor cell probability
- Modeling the therapy response
  - Response to drug.
  - Response to irradiation.
- Including more modalities and improving the model.
  - Spectroscopy
  - PET,…

Perspectives II

- Build DTI atlases from healthy subjects
  - Build Non Rigid registration algorithms for DTI
  - Statistical framework in agreement with the application
- Account for mis-registration in the inverse problem formulation
  - Add some local flexibility in the estimation process
- Build real time surgery simulators
- Use the biomechanical model for intra-operative image guided surgery

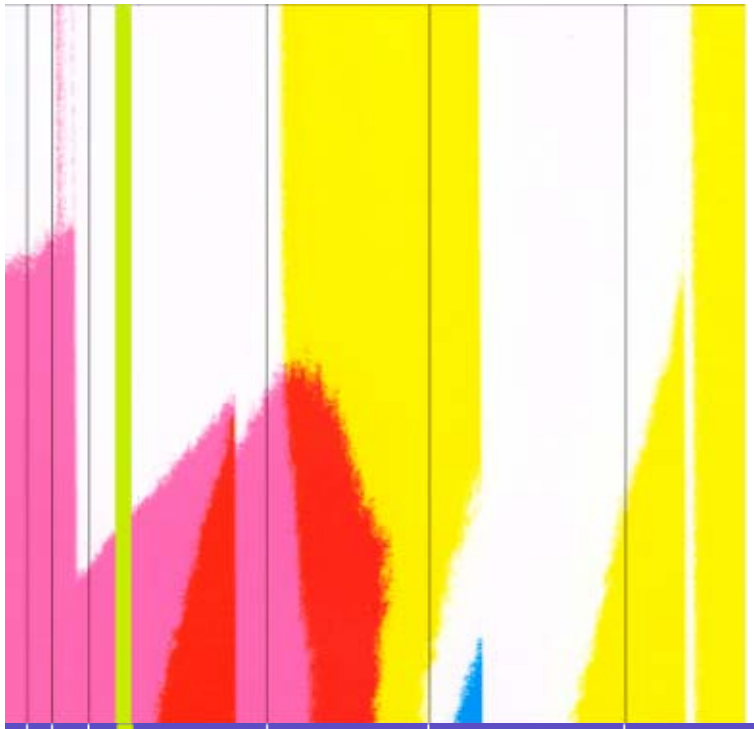

Focused ultrasound for the treatment of brain tumor

INSTITUT NATIONAL
DE RECHERCHE
EN INFORMATIQUE
ET EN AUTOMATIQUE

INRIA
SOPHIA ANTIPOLIS

Idea

Use ultrasound to burn tumors

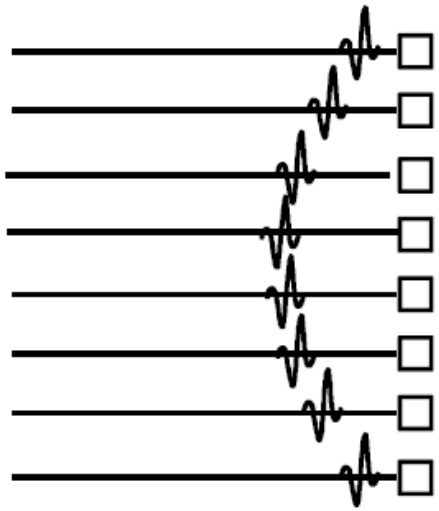

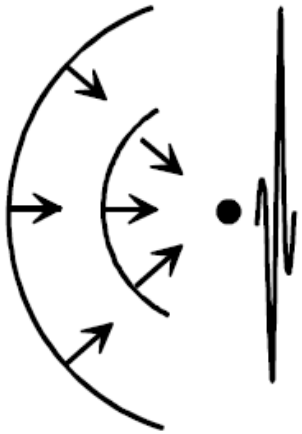

Already used for kidney and liver.

How about brain ?

Problem

- Ultrasound propagation speed is not constant through the skull !

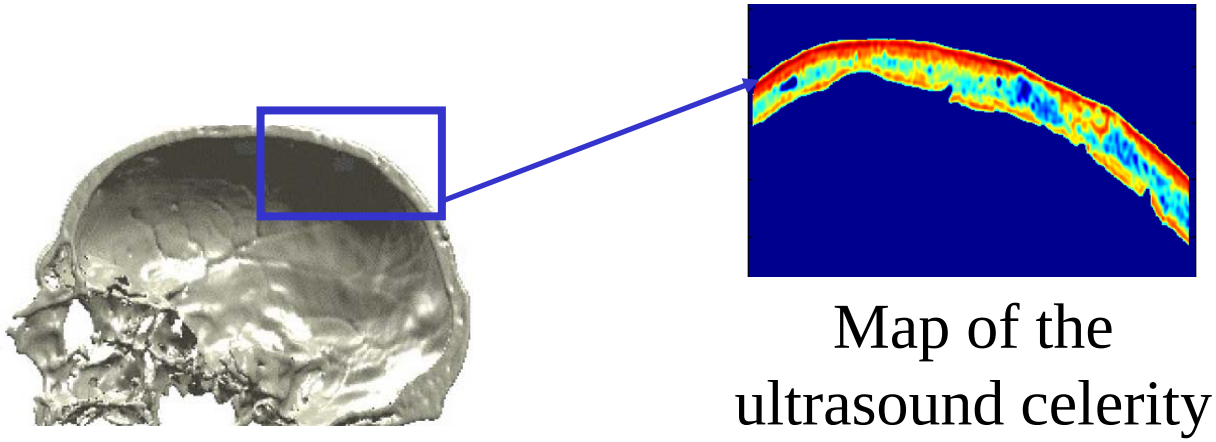

Map of the ultrasound celerity

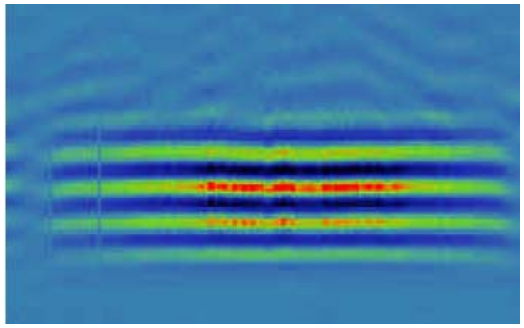

Wave propagation in water

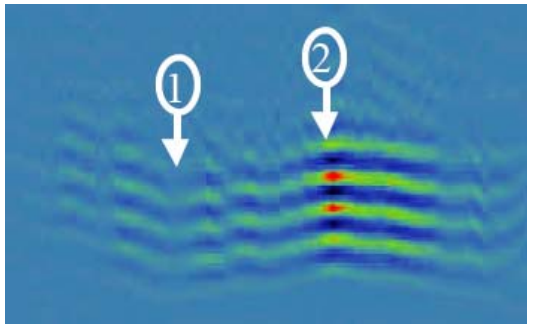

Wave propagation through the skull

First solution

$$\left(1+\tau(\vec{r})\frac{\partial}{\partial t}\right)\left[\rho_0(\vec{r})\nabla.\left(\frac{1}{\rho_0(\vec{r})}\nabla p(\vec{r},t)\right)\right]=\frac{1}{c_0(\vec{r})^2}\frac{\partial^2 p(\vec{r},t)}{\partial t^2}$$

- Neglect dispersion in the material

$$\rho(r)\,div\left(\frac{\overrightarrow{grad}\,p(r,t)}{\rho(r)}\right)-\frac{1}{c^2(r)}\frac{\partial^2 p(r,t)}{\partial t^2}=0$$

➡ reverse time !

$p(\vec{r},t)$ solution $\Rightarrow$ $p(\vec{r},-t)$ solution

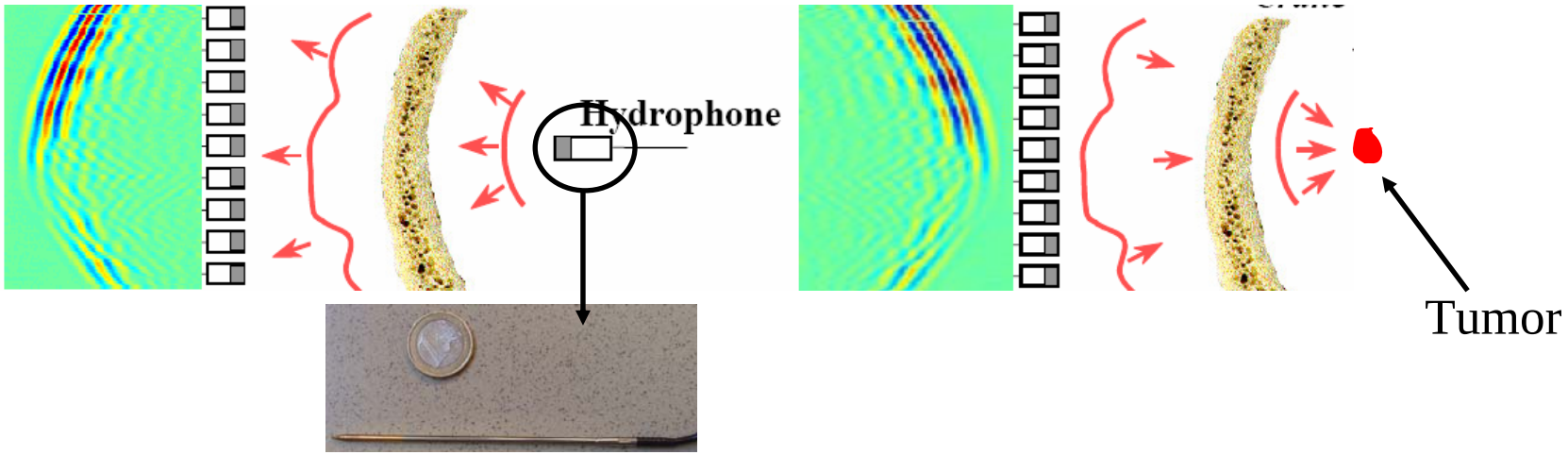

[Pernot] Mathieu Pernot. Nouvelles techniques de thérapie ultrasonore et de monitoring. *Thèse de doctorat de l'université Paris 7*. 12 Octobre 2004.

[Aubry] Jean-François Aubry. Focalisation ultrasonore adaptative : application à l'imagerie et à la thérapie du cerveau . *Thèse de doctorat de l'université Paris 7*. 18 mars 2002

Second solution

- Computational model:

$$\rho_0(\vec{r})\nabla\cdot\left(\frac{1}{\rho_0(\vec{r})}\nabla p(\vec{r},t)\right)=\frac{1}{c_0(\vec{r})^2}\frac{\partial^2 p(\vec{r},t)}{\partial t^2}$$ Ultrasound wave propagation

$$\rho C_t\frac{\partial T(r,t)}{\partial t}=k\nabla^2 T(\vec{r},t)-W_b C_b(T(\vec{r},t)-T_a)+Q_p(\vec{r},t)$$ Bio-heat equation

$$q=\frac{\alpha|p|^2}{\rho c}.$$ Coupling equation

- Inverse problem:

$$\tilde{J}(u) = \frac{1}{2}\int_0^{t_f}\left\{\|T(t)-T_{\mathrm{d}}(t)\|_{\vartheta}^2 + \sum_{k=1}^{2m} s_k\left(\frac{du(t)}{dt}\right)^2\right\}dt$$

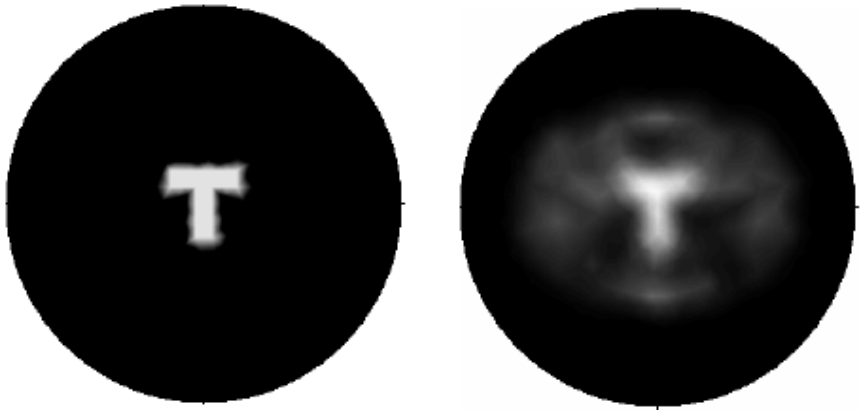

[Hynynen] X. Yin, K. Hynynen. A numerical study of transcranial focused ultrasound beam propagation at low frequency. *Phys Med Biol.* 2005 Apr 21;50(8):1821-36.

[Malinen] M. Malinen, T. Huttunen, and J. Kaipio. An optimal control approach for ultrasound induced heating. *International Journal of Control*, 76(13):1323-1336, Sept 2003.

Third solution

- MRI guided focused ultrasound

Temperature sensitive MR image

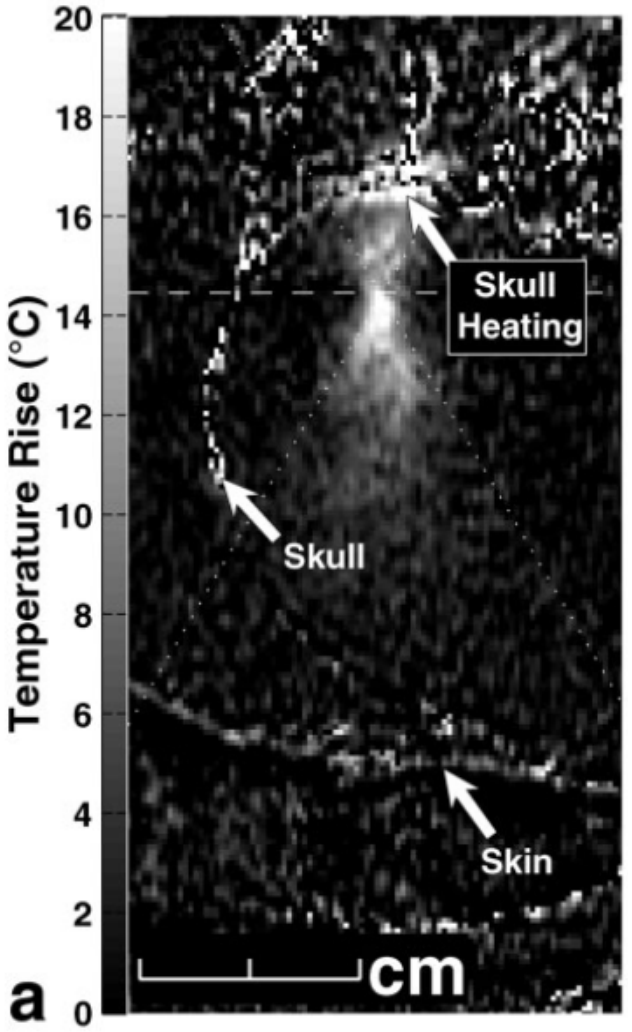

[McDannold] N. McDannold, M. Moss, R. Killiany, D. Rosene, R. King, F. Jolesz, and K Hynynen. MRI Guided Focused Ultrasound Surgery in the Brain:Tests in a Primate Model. Magnetic Resonance in Medicine 49:1188–1191 (2003).

Why is this interesting ?

- Scientific chalenges
  - Medical imaging
  - Numerical simulation
  - Inverse problem
  - Could be validated !

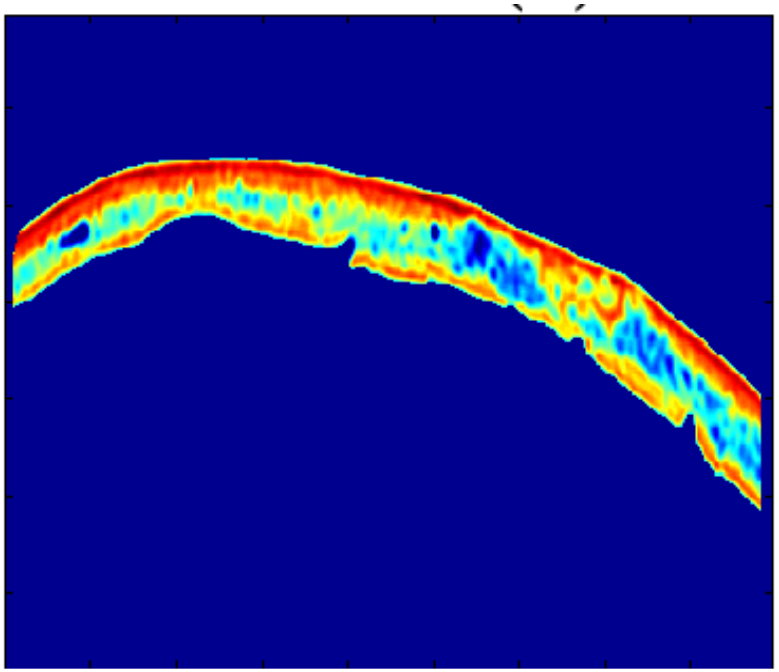

- Clinical outcomes
  - Non invasive
  - Cheaper
  - NIH agreement for human experiments (2005) (MR guided)

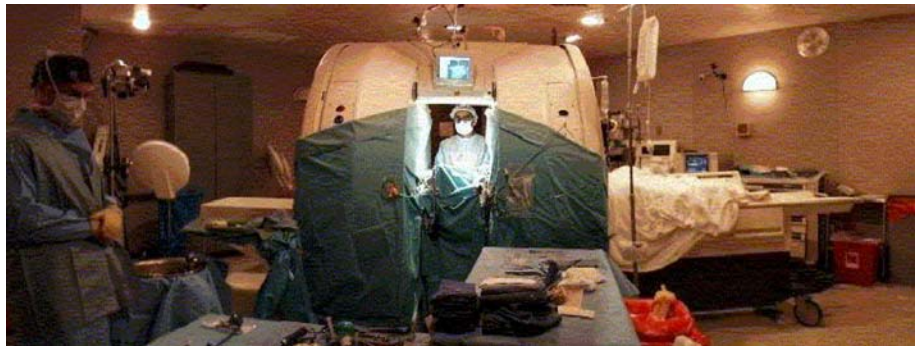

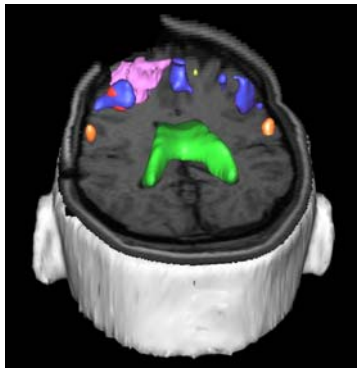

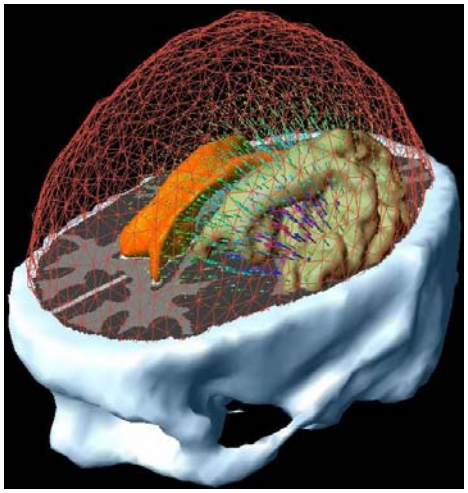

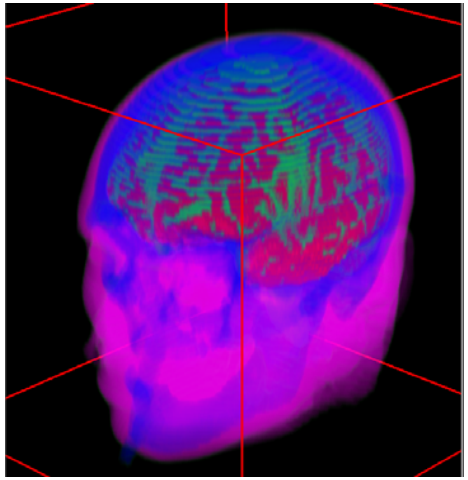

www-sop.inria.fr/asclepios/

www.clatz.com

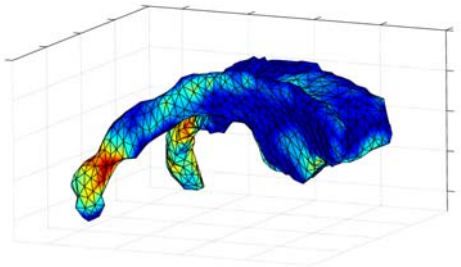

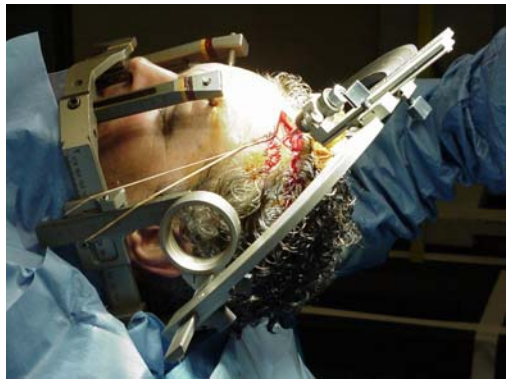

Thank you